Locally emitted fungal spores serve as high temperature ice nucleating particles in the European sub-Arctic

Jürgen Gratzl[1], Alexander Böhmländer[2], Sanna Pätsi[3], Clara-E. Pogner[4], Markus Gorfer[4], David Brus[5], Konstantinos Matthaios Doulgeris[5], Florian Wieland[1], Eija Asmi[5], Annika Saarto[3], Ottmar Möhler[2], Dominik Stolzenburg[1], and Hinrich Grothe[1]

[1]Institute of Materials Chemistry, TU Wien, Vienna, 1060, Austria
[2]Institute of Meteorology and Climate Research, Atmospheric Aerosol Research (IMK-AAF), Karlsruhe Institute of Technology (KIT), Karlsruhe, 76121, Germany
[3]Biodiversity Unit, University of Turku, Turku, Finland
[4]Center for Health and Bioresources, AIT Austrian Institute of Technology GmbH, Tulln, 3430, Austria
[5]Finnish Meteorological Institute, Atmospheric Composition Research, Helsinki, Fl-00101, Finland

Correspondence: Hinrich Grothe (hinrich.grothe@tuwien.ac.at)

Abstract.

Primary biological aerosol particles (PBAPs) can influence weather and climate by acting as high-temperature ice nucleating particles (INPs), especially in clean, rural regions like the European sub-Arctic. However, the actual contribution to atmospheric ice nucleation and exact identity of PBAPs serving as INPs remains poorly understood.

5   Here, we present measurements of INPs and highly fluorescent aerosol particles (HFAPs) over the course of one year, at the Pallas Atmosphere-Ecosystem Supersite in the Finnish sub-Arctic, aiming to determine whether PBAPs significantly contribute to atmospheric INPs and to identify which types do so. Our findings indicate that certain HFAPs are strongly influenced by meteorological variables, with high concentrations occurring when the station is within the atmospheric mixing layer, suggesting local biological sources. These HFAPs are the main contributors to high-temperature INPs, with an exceptionally

10   strong correlation (r = 0.94, p < 0.0001) between HFAP concentrations and INPs active at –13.5 °C. For the first time, we combine INP and HFAP data with direct fungal spore counts and environmental DNA (eDNA) analysis to determine the biological origins of HFAPs and INPs. Our Findings indicate that most high-temperature INPs are likely fungal spores. eDNA analysis further reveals that airborne fungi are dominated by Basidiomycota and that only a small fraction of the detected fungal genera has been tested for ice nucleation activity (INA) to date. Of those tested, most exhibit very low or no INA. This

15   underscores the significant knowledge gap in our understanding of biological ice nucleation in the atmosphere.

1   Introduction

Atmospheric aerosols are important and highly variable constituents of the atmosphere. They impact weather and climate by directly scattering or absorbing solar radiation or by changing the radiative properties and lifetime of clouds by acting as cloud condensation nuclei (CCN) or ice nucleating particles (INPs) (Masson-Delmotte et al., 2021; Pruppacher et al., 1998).

20   The latter constitute only a minor fraction of the total aerosol population (Burrows et al., 2022) and measurements of INP

concentrations remain scarce. Measuring and modeling INPs is challenging, due to their high spatial and temporal variability and the complexity of their sources (Herbert et al., 2025; Burrows et al., 2022; Welti et al., 2018). Observations of INPs are particularly rare in Arctic and sub-Arctic environments, where the temperature increase due to anthropogenic climate change is 1.5 to 4 times faster than the global average (Serreze and Barry, 2011; Cohen et al., 2014; Rantanen et al., 2022), a phenomenon

25 known as Arctic amplification. Although the ice or snow albedo effect is considered the primary driver of Arctic amplification (Screen and Simmonds, 2010), cloud feedbacks are the major uncertainties in climate projection models (Ceppi et al., 2017; Zelinka et al., 2020). Model studies indicate that the radiative properties of Arctic low-level clouds are sensitive to variations in INP concentrations (Gjelsvik et al., 2025; Xie et al., 2013), suggesting that both the concentration of INPs, and their activation temperature dependence could play a crucial role in understanding Arctic amplification (Murray et al., 2021; Tan et al., 2022).

30 In particular, the imprecise representation of biological INPs can significantly impact the overall accuracy of INP predictions in climate models (Cornwell et al., 2023).

INPs active at temperatures below -15 °C are generally dominated by mineral dust (Irish et al., 2019; Kanji et al., 2017; Murray et al., 2012; DeMott et al., 2003). Since the 1970s, biological particles, particularly bacterial cells, have been known to nucleate ice at much higher sub-zero temperatures (Maki et al., 1974; Schnell and Vali, 1976; Maki and Willoughby, 1978).

35 However, atmospheric primary biological aerosol particles (PBAPs), like fungal spores, pollen and bacteria have historically received little attention from atmospheric scientists (Kabir et al., 2020; Xie et al., 2020; Fröhlich-Nowoisky et al., 2016). More recently, emerging evidence suggests, that the majority of atmospheric INPs active above -15 °C are of biological origin, as indicated by heat sensitivity tests (e.g. Hartmann et al. (2021); Šantl Temkiv et al. (2019); O'Sullivan et al. (2018); Garcia et al. (2012); Christner et al. (2008)) and single particle fluorescence measurements (Taketani et al., 2025; Kawana et al.,

40 2024; Pereira Freitas et al., 2023; Cornwell et al., 2023; Schneider et al., 2021; Twohy et al., 2016; Mason et al., 2015; Wright et al., 2014; Tobo et al., 2013). Both techniques are valuable, but neither alone is sufficient to pinpoint the exact types of bio-INPs. Additionally, heat tests may deactivate non-biological INPs, introducing uncertainties (Daily et al., 2022). Single particle fluorescence spectrometers such as the Wideband Integrated Bioaerosols Sensor (WIBS) used in this study, currently lack the ability to reliably differentiate PBAPs without additional instrumentation. For example, a wide variety of biological,

45 natural and anthropogenic aerosols have been associated with overlapping fluorescence channels of the WIBS. An overview of fluorescent particles detected by the WIBS in field and laboratory studies can be found in Gratzl et al. (2025).

To investigate what types of PBAPs exhibit ice nucleation activity (INA), several laboratory studies have been conducted. INA has been identified in pollen from phylogenetically diverse plants (Pummer et al., 2012; Diehl et al., 2001) and pollen constituents (Augustin et al., 2013; Pummer et al., 2015; Burkart et al., 2021; Matthews et al., 2023; Wieland et al., 2025).

50 Additionally, numerous strains of ice nucleation active bacteria have been isolated from clouds or precipitation (Failor et al., 2017; Šantl Temkiv et al., 2015; Joly et al., 2013; Stephanie and Waturangi, 2011). Less is known about the INA of fungal spores. Only a small fraction of known fungal species or genera have been tested for INA, and only a handful of them nucleate ice above -15 °C (Fröhlich-Nowoisky et al., 2015; Haga et al., 2014, 2013; Morris et al., 2013; Pummer et al., 2013; Huffman et al., 2013; Pouleur et al., 1992; Jayaweera and Flanagan, 1982). Ascomycota (sac fungi) and Basidiomycota (club fungi) are

55 the two major Phyla of fungi. Among those fungi tested for INA, most belong to the Ascomycota. However, a high abundance

and diversity of Basidiomycota is expected in the atmosphere (Niu et al., 2024; Maki et al., 2023; Qu et al., 2021; Huffman et al., 2013). In the boreal forest which spans large areas of the sub-Arctic, Basidiomycota could dominate over Ascomycota (Qu et al., 2021; Sterkenburg et al., 2015). Given the vast diversity of fungal species many of which remain uncharacterized for INA, their potential role in atmospheric ice nucleation remains largely unknown. Recent studies have shown that terrestrial environments serve as important sources of biological high temperature INPs in the Arctic and sub-Arctic. INPs active above -15 °C exhibit a pronounced seasonality, peaking in summer during snow and ice free periods (Barry et al., 2025; Tobo et al., 2024; Pereira Freitas et al., 2023; Schneider et al., 2021; Wex et al., 2019). Fu et al. (2013) and Pereira Freitas et al. (2023) observed similar seasonal cycles in arabitol and mannitol, chemical tracers of fungal spores (Bauer et al., 2008), which they also contributed to terrestrial sources.

These findings imply that high temperature INPs may become more prevalent in a warming climate, due to arctic greening and prolonged snow free periods in the northern boreal forest (Barry et al., 2025; Berner et al., 2020; Tobo et al.; Dankers and Christensen, 2005) and that fungal spores might contribute significantly to the highly active INP population. More data on the concentration and biological origin of high temperature INPs in northern latitudes could enhance our understanding of cloud feedback mechanisms and potentially improve present and future climate predictions. Given the vast extent of the boreal forest, it should be considered a potentially critical source of biological INPs. Here, we hypothesize that locally emitted fungal spores from the northern boreal forest are the dominant source of high-temperature INPs in the European sub-Arctic. We present measurements of INPs and PBAPs from the Pallas Atmosphere-Ecosystem Supersite. We combine single particle fluorescence measurements with direct fungal spore counts and complement these data with eDNA sequencing of airborne fungi to elucidate the biological origin of high temperature INPs in this region.

2   Methods

2.1   Observation site

Measurements were conducted at Sammaltunturi station at the Pallas Atmosphere-Ecosystem Supersite in Finnish Lapland within the Pallas-Yllästunturi-National Park. Pallas is located 170 km north of the Arctic Circle, at the northern edge of the boreal forest, and experiences a sub-Arctic climate (Köppen, 1931; Beck et al., 2018). Sammaltunturi station (67.9733° N, 24.1157° E) is situated on top of Sammaltunturi hill at an elevation of 565 meters above sea level, approximately 100 meters above the treeline. As a result, vegetation in the immediate vicinity consists primarily of low vascular plants and lichen (Hatakka et al., 2003). The air at Pallas is considered representative of the clean continental background air of northern Europe, as there are minimal local or regional air pollution sources (Doulgeris et al., 2022; Lohila et al., 2015).

2.2   Setup and timeline

The campaign took place in two parts: The first part was integrated into the Pallas Cloud Experiment 2022 (PaCE22) campaign (Brus et al., 2025) from September to December 2022 and the second part of the campaign was from April to September 2023.
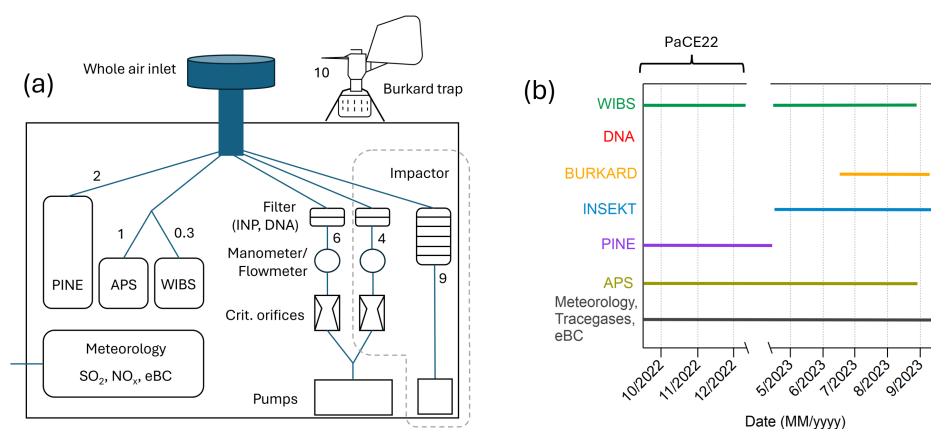
Figure 1. (a) Setup of used instruments at Sammaltunturi station. On rooftop: Burkard trap, inside all other instruments. The number beside the instruments indicate the flow rate in $l\,min^{-1}$. (b) Timeline of when the specific instruments (or filter loading for subsequent analysis) were operated during the campaign.

The instruments were operated at either one or both parts of the campaign. The times when each instrument was operated is shown in In Fig.1 (b). Additionally to the instruments described in sect. 2.3 to 2.8, an Aerodynamic Particle Sizer APS 3321 (TSI, USA) was operated at the station and was used to confirm meaningful data collection by the WIBS (see Supplement Sect. 1). The setup can be seen in Fig.1 (a). The Numbers beside the instruments refer to the flow rate ($l\,min^{-1}$). The main inlet for aerosol instruments at the Sammaltunturi station is a whole air inlet with no cut-off diameter and thus collecting aerosols effectively also during fog and in-cloud periods. The inlet is located 2 m above the station's roof and approximately 6m above ground. The inlet is slightly heated to avoid snow and ice accumulation outside when the station is inside clouds or when it is snowing. The aerosol instruments connected to the inlet have separate Permapure MD-700 nafion dryers for sample drying. More details about the inlet and sampling can be found in Backman (2025). All concentrations, except for the Burkard trap are reported for standard conditions. If not explicitly written otherwise, all data is reported in Eastern European Time (UTC+2h), which is used as station time in Sammaltunturi.

2.3 Single particle fluorescence measurement

A Wideband Integrated Bioaerosol Sensor 5/NEO (WIBS, Droplet Measurement Technologies, USA) was used to measure total aerosol particle (TAP) and highly fluorescent aerosol particle (HFAP) concentrations, as well as size distributions from 0.5 to 30 µm. The WIBS is a light induced fluorescence (LiF) sensor that enables the measurement of auto-fluorescence in individual aerosol particles. The instrument operates with an inlet flow rate of $0.3\,l\,min^{-1}$, directing air through an aerodynamic lens. A 635 nm laser measures particle size and shape and serves as a trigger for two UV-Xenon lamps. These lamps excite particles at wavelengths of 280 nm and 370 nm, with fluorescence subsequently detected by two detectors at wavelength ranges of

310–400 nm and 420–650 nm. This results in three fluorescence channels: FL1 (excitation at 280 nm, emission at 310 - 400 nm), FL2 (excitation at 280 nm, emission at 420-650 nm) and FL3 (excitation at 370 nm, emission at 420-650 nm). A forced trigger measurement is used to identify the fluorescence background, without any particles present in the scattering volume. The forced trigger measurement was done every 6 hours for 1 minute to account for a possible shift in the background. Here, an aerosol particle is labeled as highly fluorescent (HFAP) if it exceeds the threshold TH, calculated by

$$TH = \overline{FT} \times 9\sigma \tag{1}$$

in any channel, where $\overline{FT}$ is the mean value of the forced trigger intensity and σ is the standard deviation of the same. Using Perring nomenclature (Perring et al., 2015), one can define 7 fluorescent particle types, depending on the combination of channels exceeding the threshold: A particles are fluorescent in FL1 only, B particles in FL2 only and C particles in FL3 only. AB particles are fluorescent in FL1 and FL2 only, AC particles in FL1 and FL3 only, BC in FL2 and FL3 only and ABC particles are fluorescent in all three channels. The approximated shape of particles is calculated via an analysis of the forward scattered light in 4 quarters of the quadrant photo multiplier tube and described by the asymmetry factor AS, a dimensionless number between 0 and 100, where a hypothetical perfect sphere should yield the value 0 and and a thin fiber should yield a value close to 100 (Gabey et al., 2010). Data acquisition, processing and quality control is described in detail in Gratzl et al. (2025) for data collected during the PaCE22 campaign, and was handled in the same way for the second part of the campaign. In Gratzl et al. (2025), an overview of particles that have been associated with the different fluorescent particle types in laboratory and field studies can be read as well.

2.4 Ice nucleating particle measurements

2.4.1 INSEKT

The Ice Nucleation Spectrometer of the Karlsruhe Institute of Technology (INSEKT) is an offline-based instrument to investigate the freezing ability of aerosol particles down to -25 °C. 47 mm polycarbonat filters (Whatman®) with 0.2 µm pore size were installed in a metal filter housing down the TSP inlet (see Fig. 1) and changed once a week or more often. Loaded filters were removed from the filter housing, placed into sterile petri dishes and stored in a freezer. The filter handling is described in detail in Böhmländer et al. (2024). The flow rate was held constant at $6.0\,\mathrm{l\,min^{-1}}$ using a critical orifice and a pump. Filters were transported to Germany in a cooled styrofoam box and upon arrival stored in a freezer at -20 °C until analysis. Aerosol suspensions are created by inserting loaded filters into a polycarbonate tube filled with Nanopure™ water and subsequent rotating (Schneider et al., 2021). The aerosol suspension is split into 50 µl aliquots and filled into PCR trays. The PCR trays are cooled at a rate of $0.33\,\mathrm{K\,min^{-1}}$ and the greyscale of each aliquot is observed with a camera. A sudden drop in the greyscale value signals the occurrence of a freezing event, leading to a fraction of frozen aliquots as a function of temperature. The INP concentration is calculated from this frozen fraction according to Vali (1971), whereas the uncertainty originates from Agresti and Coull (1998). A Nanopure water background is always present in each experiment, limiting the minimal temperature to -25°C. INSEKT is based on the Colorado State University - Ice Spectrometer (Hill et al., 2016) and additional technical details are given in Schneider et al. (2021).

The aerosol suspensions were - in addition to a standard analysis - subjected to a heat treatment to disable the ice nucleating ability of heat-labile INPs at 95 °C for 20 minutes. These heat-labile INPs are typically of biological origin, allowing a better understanding of the INP population present during filter sampling Schneider et al. (2021).

2.4.2 PINE

The Portable Ice Nucleation Experiment (PINE) is an expansion-type cloud chamber with a volume of 10 l (Möhler et al., 2021). Inside an expansion-type cloud chamber, the pressure is decreased rapidly, leading to a near-adiabatic decrease in temperature due to expansion cooling, while the relative humidity increases. If aerosol particles are present, they are able to act as CCN and/or as INP, leading to the formation of cloud droplets and/or ice crystals. The chamber can be operated between -60 and -10 °C to measure in the mixed-phase regime (> -35 °C) as well as the cirrus regime (< -35 °C). The cloud droplets and ice crystals are detected optically with an optical particle counter (OPC). During analysis they are divided by their optical size, and the number of ice crystals is counted, representing the number of INPs. An expansion is performed every six minutes, leading to a high temporal resolution of the INP concentration. The PINE is an autonomous instrument that can be controlled remotely via a custom-made LabVIEW program. This dataset is described in more detail in Böhmländer et al. (2025).

2.5 Burkard Spore trap

Pollen and fungal spores were monitored with a Burkard 7-day volumetric sampler (short Burkard trap, Burkard Manufacturing Co. Ltd., UK; (Hirst, 1952)). The sampler was located on an open corridor on the rooftop of Sammaltunturi station approximately 3 meters above ground. The sampling and analyzing methods followed the standard methodology adopted by the Finnish pollen information network following the principles of the European Aeroallergen Network (https://ean.polleninfo.eu/info/en/). The air suction volume of the Burkard sampler was, on average, $10 \, \mathrm{l \, min^{-1}}$. Airborne particles were trapped on a Melinex tape coated with an adhesive (Vaseline and paraffin wax mixture). The tape was attached to a clockwork device, which rotated at the rate of $2 \, \mathrm{mm \, h^{-1}}$. After sampling, the tape was cut into pieces representing one single day each. These pieces were mounted on slides with Gelvatol under a cover glass. Pollen grains and some plant and fungal spores were counted from the samples using optical microscopy. Pollen grains were identified to Family or Genus level. Spores were counted, if the identification to the taxonomic group, where the recognition could be done reliably, was possible. These are hereinafter referred to as identifiable fungal spores and identifiable plant spores, or identifiable spores if both are meant. In addition, from three separate days, total number of all fungal spores were counted (even if they could not be assigned to any higher taxonomic level). The spores were divided into two groups: a) particles that could be reliably identified to be fungal spores and b) a group where the identification was slightly uncertain, but particles were believed to be fungal spores. Both together are referred to as total fungal spores. The concentrations of the pollen grains, plant spores and fungal spores of each taxa were determined by random sampling of microscopic fields, with a time accuracy of 2 hours (Mäkinen, 1981). In the end, the pollen and spore counts were converted to daily averages per cubic meter of air.

2.6 eDNA Sequencing

170 For eDNA Sequencing of airborne fungi, 47 mm polycarbonat filters (Whatman®) with 0.2 μm pore size were installed in a metal filter housing and changed twice a day for 4 days, resulting in 8 filters. Loaded filters were removed and stored in a freezer. The filter holder was cleaned carefully with Isopropanol before a new filter was installed. The flowrate was recorded at all times and held constant at $4\,\mathrm{l\,min^{-1}}$ using a critical orifice and a pump. Filters were transported to Austria in a cooling box and instantly upon arrival put in a freezer at -20 °C, until brought to AIT for eDNA analysis.

175 For DNA extraction filters were dissolved in 750 μl Phenol/Chloroform/Isoamylalcohol solution. Subsequently, 750 μl buffer AP1 from Plant Mini-Kit (Qiagen) was added to the organic solvents. The mixture was vigorously vortexed and centrifuged at 13000 rpm for 10 min. The aqueous phase was removed and mixed with 400 μl P3. All further steps followed the manufacturer's protocol. At the end, DNA was eluted with 50 μl AE. Library preparation and high-throughput sequencing was done at LGC (Berlin, Germany). The fungal ITS2-region was amplified with primer pair ITS3Mix/ITS4Mix (adapted from Tedersoo et al. (2014) as outlined in Gorfer et al. (2021)) containing Illumina TrueSeq adapters. Reaction mixtures contained 15 p mol of each forward and reverse primer in 20 μl volume of 1 × MyTaq buffer containing 1.5 units MyTaq DNA polymerase (Bioline GmbH) and 2 μl of BioStabII PCR Enhancer (Sigma-Aldrich). The first amplification of the two-step PCR approach ran for 30 cycles: 1 min 96 °C pre-denaturation followed by 15 s at 96 °C denaturation, 30 s at 58 °C annealing and 90 s at 70 °C extension and a final hold at 8 °C. The second amplification was as the previous amplification but with standard i7- and i5-

185 sequencing adapters and with modified annealing temperature, i.e. 3 cycles at 50 °C followed by 7 cycles at 58 °C. DNA concentration of amplicons was assessed by agarose gel electrophoresis. About 20 ng of indexed amplicon DNA of each sample was subsequently pooled. The pooled libraries were purified with one volume of Agencourt AMPure XP beads (Beckman Coulter) to remove primer dimer and other small mispriming products, followed by an additional purification on MiniElute columns (Qiagen). The size selection was performed by preparative gel electrophoresis on an LMP-Agarose gel. Sequencing

190 was done on an Illumina MiSeq using V3 Chemistry (2 × 300 bp). Downstream bioinformatic analyses of raw paired end reads obtained from MiSeq V3 runs were done as previously described (Gorfer et al., 2021). Initial quality filtering was done with Trimmomatic v. 0.39 (Bolger et al., 2014). USEARCH program suite (Edgar, 2010) was used for merging the forward and reverse reads with a minimal overlap of 30 bp with fastq_mergepairs. Sequences < 280 bp were all of non-fungal origin and thus filtered out. FASTX toolkit script fastx_barcode_splitter.pl was used to sort out project-specific fungal sequences; USE-

195 ARCH scripts were used for chimera detection and filtering underrepresented sequences (< 10). VSEARCH (Rognes et al., 2016) was used for clustering and counting sequences per cluster, using a 97 % sequence similarity, which is a widely used threshold for the ITS region and lies between generally accepted limits for discrimination of species and genera (Vu et al., 2019). OTU clustering instead of using 100 % identical amplicon sequence variants (ASVs) was recommended for fungal ITS datasets (Tedersoo et al., 2022). Taxonomic affiliation of OTUs was done with the UTAX script against the UNITE database

200 (Abarenkov et al., 2024). Non-fungal sequences were removed from further analyses. All sequence affiliations were manually evaluated and edited, increasing the phylogenetic accuracy (Hofstetter et al., 2019). Given the set sequence similarity threshold, species names provided for OTUs must be considered sensu lato. Further bioinformatics and statistical analyses were done in R

version 4.3.1 (cran.r-project.org) with the following packages: vegan (Oksanen et al., 2018), phyloseq (McMurdie and Holmes, 2013), metagMisc (Mikryukov and Mahé, 2025) and microViz (Barnet, 2024).

205   Most samples had read numbers for fungi clearly above 3000, but the two samples from the last sampling day had only 815 and 685 reads, respectively. To allow inclusion of these two samples, for further analyses, all samples were rarefied to 685 reads with the function rarefy_even_epth in phyloseq. Retrieval of relative abundances of specific taxa was done by converting the read numbers to relative abundances, agglomerating taxa at the appropriate level (tax_glom in phyloseq) and seleceting desired taxa (subset_taxa in phyloseq) or selecting most abundant taxa (phyloseq_filter_top_axa in metagMisc).

2.7   Impactor measurements and fluorescence microscope

210

An impactor (Sioutas Five-stage Cascade Impactor, SKC, US) was installed down the whole air inlet in parallel to filters for eDNA analysis (see Fig. 1) and was operated at $9 \, \mathrm{l \, min^{-1}}$ using a Leland Legacy Personal Sampling Pump (LKC, USA). The flow was checked every day and if necessary calibrated. Aluminum foil (cleaned with aceton and baked at 300 °C for at least 5 h) was installed in four stages (cut-off dimaters: 2.5 μm, 1 μm, 0.5 μm, 0.25 μm aerodynamic diameter (Da)). After

215   each sampling period, the aluminum foils were removed and stored in a freezer. The impactor was cleaned before a new set of foils was installed. The foils were analyzed with a Nikon Eclipse Ci-L microscope (Nikon, Japan) under bright field and fluorescence setting (λ_{ex}=465-495 nm, λ_{em}=515-555 nm).

2.8   Meteorological variables and air pollutants

The Sammaltunturi station is equipped with Vaisala Milos 500 automatic weather station. The wind speed was measured with

220   a heated cup anemometer and the wind direction with a heated wind vane. Temperature was measured with Pt100 sensors and relative humidity with a Vaisala sensor (HUMICAP). Visibility was measured by a Vaisala FD12P present weather sensor. Data is saved as one minute means (Hatakka et al., 2003).

    The equivalent Black Carbon (eBC) concentration in Sammaltunturi is measured optically with an AE-33 Aethalometer (Magee Scientific) instrument connected to the whole air inlet. The instrument measures how light is attenuated as it passes

225   through a filter loaded with particles, which converts to aerosol absorption. The aerosol absorption is used to estimate the eBC mass, assuming a default, constant mass absorption cross-section (MAC) of $7.77 \, \mathrm{m^2 \, g^{-1}}$ at 880 nm and a filter-tape correction of 1.39 (Drinovec et al., 2015). AE33 features a dual-spot configuration, analyzing two filter spots with differing airflow rates at the same time. Additionally, a reference spot, unaffected by the sample flow, is used to monitor any fluctuations in the light source's intensity. To ensure measurement reliability, the instrument performs regular zero-flow and optical calibrations. Once

230   the attenuation value reaches 120, it automatically advances to a filter spot.

    The gas compositions in Sammaltunturi are measured through a common sampling inlet line with a flow of about $90 \, \mathrm{m^3 \, h^{-1}}$ and a residence time of two seconds (Hatakka et al., 2003). A chemiluminescence analyzer with molybdenum converter, Thermo Environmental Instruments 42 CTL (TEI42CTL), is used to measure NO_2 concentrations. At Sammaltunturi station, the NO_2 concentration measured by TEI42CTL is a sum of all oxidized nitrogen species. However, NO_x concentration levels

235   at Pallas are low, especially during summer. Thus, the results are most of the time below the instrument detection limit (50

ppt). Analysis of SO_2 is based on measuring UV fluorescence. The instrument used is Thermo Environmental Instruments 43S. Details on air pollutant monitoring can be found in Hatakka et al. (2003).

2.9 Air mass back trajectories

Air mass back trajectories were carried out using the NOAA HYSPLIT Trajectory Model v5.3.0 (Stein et al., 2015; Rolph
240 et al., 2017), using meteorological data from the Global Data Assimilation System (GDAS) archive (1 degree resolution). 72 hours back trajectories were calculated for air masses arriving either 100 m or 500 m above ground level at Sammaltunturi station.

3 Results and Discussion

3.1 The contributions of different HFAPs changes seasonally

245 Figure 2 provides an overview of the monthly fractions of HFAPs within TAPs, ambient temperature (measured at Sammaltunturi), and and the relative contributions of different fluorescent particle types to HFAPs. The fractions of HFAPs exhibit a clear seasonal trend. At the start of the PaCe22 campaign in September 2022, the median fraction is 5.6×10^{-2} and steadily decreases until the end of the PaCE22 campaign in December 2022, when the minimum monthly median value of 6.5×10^{-3} is reached. From April to August 2023, the HFAP fraction increases continuously, peaking in August at 7.2×10^{-2}. The logarithm
250 of the fraction roughly follows ambient temperature trends (depicted in red), with minima and maxima occuring in December 2022 and August 2023, respectively. Figure 2 (b), illustrates the montly contributions of different fluorescent particle types to HFAPs. The fractions of AB and ABC particles follow the seasonal trend of temperature and total HFAP fraction. During warmer months, AB and ABC particles dominate, accounting for 60 % of HFAPs in September, 67 % in July and 75 % in August. In contrast, their contribution drops to 12 % in December. Conversely, B particles (and to a lesser extent BC particles)
255 show an inverse pattern, dominating during colder months. The contribution of A particles does no exhibit a clear seasonal trend. In the following, we will focus on AB and ABC particles, since their high contribution during warmer months suggests an biological influence on their concentration. The contributions of C and AC particles are negligibly small and will not be discussed further. (Details on A, B, and BC particles are provided in the Supplement in Sect. 2).

3.2 Local snow cover influences the concentration of biological HFAPs

260 Figure 3 shows the daily mean concentrations of TAPs, HFAPs, AB, and ABC particles. Snow depth and ambient temperature, measured at the Kenttärova research station (approximately 5.5 km east of Sammaltunturi), are also depicted in Figure 3 (a). The temperature is used to define meteorological seasons (see Supplement Sect. 2 for seasonal definitions, particle concentrations, and size distributions of all fluorescent particle types).

TAPs show no clear seasonal trend (Fig. 3 (b)). The lowest median TAP concentration occurs in autumn ($0.28 \ \mathrm{cm}^{-3}$),
265 while the highest is in summer ($0.75 \ \mathrm{cm}^{-3}$). In contrast, HFAP concentrations exhibit a strong seasonal cycle, peaking in
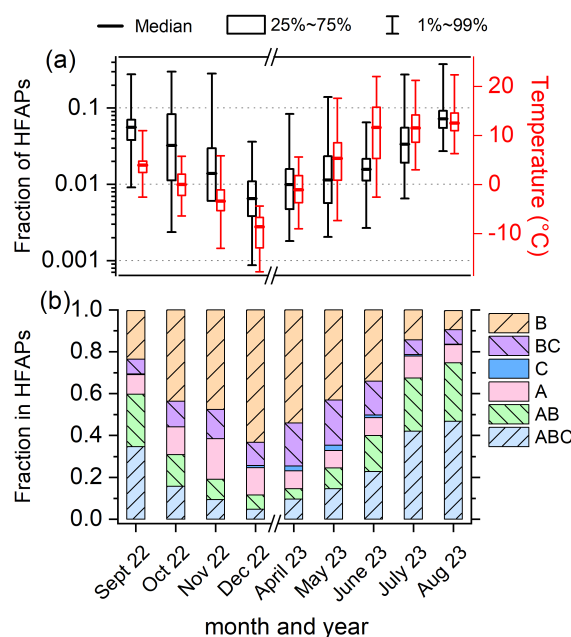
Figure 2. Overview of fraction of HFAPs and ambient temperature. (a) Monthly box diagrams (median, 25th to 75th percentile and first to 99th percentile) of the fraction of total HFAPs in TAPs and temperature. Boxplots are based on hourly mean values. (b) Monthly contributions of HFAP types to total HFAP concentration (fraction of median values). AB and ABC particles dominate in the warmer months, while B and BC particles dominate in the colder months.

summer with a median of 3.0×10^{-2} cm^{-3}, approximately 10 times higher than in winter. Winter and spring peaks of HFAPs are primarily due to B and BC particles, with A particles playing a minor role (details in Supplement Sect. 2). AB and ABC particle concentrations follow a similar pattern, suggesting a common biological origin. These particle types show the strongest seasonal cycle, with minimum median concentrations in winter (2.0×10^{-4} cm^{-3}) and maxima in summer (5.8×10^{-3} cm^{-3}

270 and 9.5×10^{-3} cm^{-3} for AB and ABC, respectively).

Snow cover significantly affects AB and ABC particle concentrations. Once the ground is covered in snow (from October 23 to May 22), concentrations decrease rapidly and remain low. For instance, the median ABC concentration in autumn (4.4×10^{-3} cm^{-3}) drops 22-fold in winter. This strongly suggests, that snow cover suppresses the emission of AB and ABC particles from the local biosphere. Once the snow begins to melt, concentrations gradually increase. Peaks in AB and ABC concentrations

275 during the melting period correspond to air masses passing over snow-free land north of the Gulf of Bothnia, such as Ylitornio Meltosjärvi (66.5333°E, 24.65° E). This suggests that regional biosphere emissions south of Sammaltunturi contribute to increased concentrations (details in Supplement Sect. 3.3). A notable example occurred on November 5, 2022 (labeled (1) in Fig. 3). On this day—the third in a three-day melting period—snow depth (measured at 8 am local time) decreased from 9.0 ± 2.0 cm to 3.3 ± 2.0 cm. Air masses on this day arrived from the south and spent most of the time close to the ground,
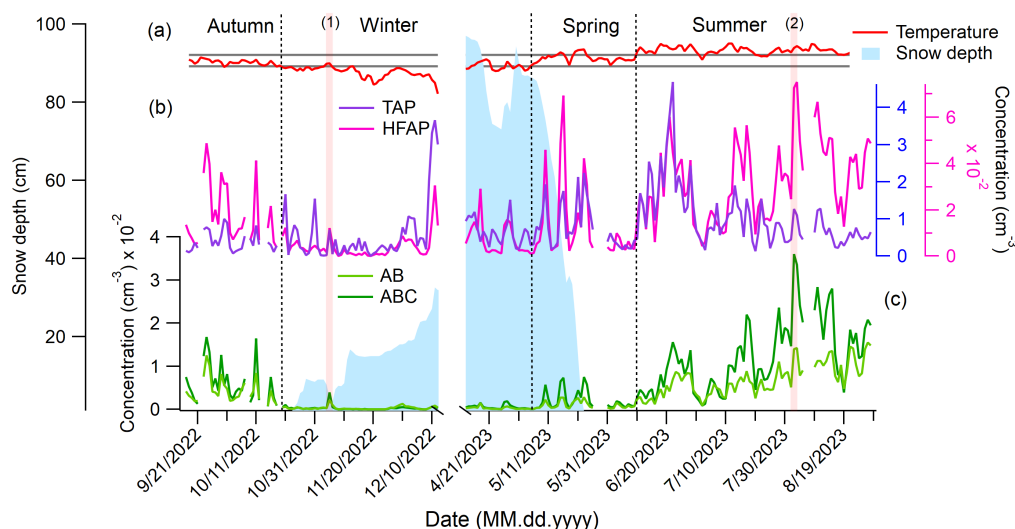
Figure 3. Daily mean concentrations of TAPs and HFAPs, as well as AB and ABC particle types, mean snow depth and ambient temperature inside a near spruce forest. (a) Temperature measured at Kenttärova station is used to define the meteorological seasons. Grey lines are at 0 °C and 10 °C. (b) TAPs and HFAPs, (c) AB and ABC particles. Horizontal transparent red lines are labeled with a number and mark certain the two days discussed in the text. Snow cover reduces the concentration of AB and ABC particles drastically.

280   following similar trajectories to the days before and after. However, in areas slightly south of Pallas, such as Kolari Kattilamaa (70 km south), snow had completely melted. This lead to an sudden 10-fold increase in ABC concentrations compared to previous two days, indicating that local emissions of AB and ABC particles resumed immediately after snow melt (details in Supplement Sect. 3.1). Days of maximum AB and ABC concentrations always correspond to local air masses near the ground (e.g., August 2, which recorded the highest daily mean value, labeled (2) in Fig. 3, see Supplement Sect. 3.4 for details). This

285   further supports the hypothesis that AB and ABC particles originate mostly from the local biosphere.

      Similar relationships between fluorescent particles and snow cover have been reported in the boreal forest. Schumacher et al. (2013) observed this phenomenon in Hyytiälä, southern Finland, using a UV-APS (TSI, USA) instrument with a fluorescence channel similar to FL3 in WIBS. At the same site, Schneider et al. (2021) found that AB and ABC particles exhibited the strongest seasonal trends, strongly influenced by snow cover. Petersson Sjögren et al. (2023) reported a comparable seasonal

290   trend in a managed coniferous forest at the Hyltemossa research site in southern Sweden using a Biotrak sampler (TSI, USA). This instrument, which operates with similar excitation and emission wavelengths ($\lambda_{ex} = 405$ nm, $\lambda_{em} = 405 - 600$ nm, D > 1 μm) as the FL3 channel in WIBS, recorded concentrations similar to those measured in this study. Since C and AC concentrations are negligible small, FL3 is primarily composed of BC and ABC particles. In autumn, the concentrations in Hyltemossa and Pallas (FL3) are 5×10^{-3} and 6×10^{-3} cm^{-3}, respectively. In winter, they are 3×10^{-3} and 7×10^{-4} cm^{-3},

295   in spring, they are 3×10^{-3} and 2×10^{-3} cm^{-3} and in summer, they are 1.3×10^{-2} and 1.4×10^{-2} cm^{-3}.
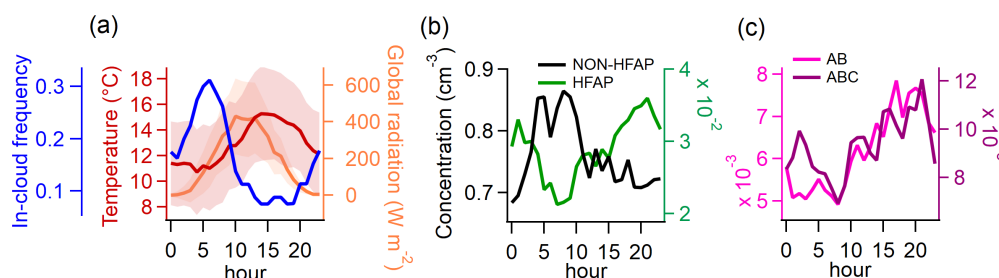
Figure 4. Diurnal patterns of meteorological parameters and particle concentrations in summer for times in which the station was not exposed to clouds. (a) Temperature, global radiation and frequency (or probability) of the station being inside a cloud (used as a proxy for probability of the station being in the free troposphere). (b) Concentration of NON-HFAPs and HFAPS. (c) Concentration of AB and ABC particles. Similarities between in-cloud frequency and NON-HFAP concentration suggest a higher contribution of far-range transport to NON-HFAP concentration. The opposite behavior of HFAP concentrations suggests locally sourced bioaerosols are the major contributors to HFAP concentrations.

3.3 Diurnal patterns reveal the coupling to the local surface

Summer-time diurnal median values were calculated only for periods when the station was outside of clouds (defined as visibility > 1000 m), as in-cloud measurements result in a considerable reduction of TAPs and HFAPs (with the former declining much more sharply, see Supplement Sect. 4). The frequency of the station being inside clouds follows a distinct diurnal cycle
300 (Fig. 4, (a), blue line) peaking at 5 am and reaching a minimum between 2 pm and 7 pm. This diurnal pattern of in-cloud frequency provides insights into whether the station is inside or outside the mixing layer at different times of the day. When cloud frequency is high at Sammaltunturi station (565 m), it is more likely that the station is inside or above the boundary layer and therefore decoupled from the local biosphere. This aligns with findings by Aalto et al. (2002), who reported temperature inversions between Pallasjärvi station (303 m) and Sammaltunturi from 9 pm to 6 am, whereas daytime typically lacked in-
305 versions. Data from the Sodankylä observatory, 125 km southeast of Pallas, show that the mixing layer in summer afternoons usually extends to 1000-1500 m (Aalto et al., 2002).

The diurnal cycle of NON-HFAPs (TAPS - HFAPs) (Fig. 4 (b)) roughly follows in-cloud frequency trend, suggesting that the highest concentrations occur when the station is in the free troposphere. In contrast, HFAP concentrations (Fig. 4 (b)) increase steadily from 7 am, peaking at 9 pm, indicating that HFAPs are most abundant when the station is within the mixing
310 layer. A similar diurnal pattern was observed by Petersson Sjögren et al. (2023) in a coniferous forest in the south of Sweden. AB and ABC particle concentrations (Fig. 4 (c)) show a delayed increase with temperature, peaking between 3 pm and 9 pm, following the general trend of HFAPs. This further supports the assumption that PBAPs originate from the local surface, with long-range transport playing a minor role in PBAP distribution. Similarly, Gao et al. (2024) found significantly higher HFAP concentrations within the planetary boundary layer than in the free troposphere at Mount Helmos in the eastern Mediterranean.

3.4 HFAPs are influenced by meteorology and air pollution

To determine whether HFAP concentrations are primarily controlled by natural meteorological variables or anthropogenic influences, Pearson correlation analysis was conducted on hourly mean WIBS data, meteorological parameters (temperature, relative humidity (R.H.)), elemental black carbon (eBC), and NO_x. Results are shown in Fig. 5 (a), with only Pearson r-values (from now on r) corresponding to p-values < 0.05 presented.

TAP concentrations show no strong correlation with temperature, R.H. or NO_x, but exhibit a correlation with eBC mass concentration (r = 0.6). Similarly, HFAP concentrations correlate with eBC concentrations (r = 0.61) but also show a weak positive correlation with R.H. and a moderate correlation with NO_x (r = 0.42) for out-of-cloud periods. HFAP concentrations also correlate with temperature (r = 0.61).

AB and ABC concentrations show correlations of 0.60 and 0.59, respectively, with temperature. This correlation strengthens when considering the common logarithm of ABC particle concentration, yielding an r-value of 0.82 (p < 0.0001) (Fig. 5 (b)). A similar logarithmic relationship is observed for AB particles, with an r-value of 0.78 (p < 0.0001). This relationship aligns with previous findings that biological activity in the atmosphere increases with temperature over seasonal time scales (e.g. Pereira Freitas et al. (2023); Petersson Sjögren et al. (2023); Schumacher et al. (2013)). A weak positive correlation between R.H. and ABC (r = 0.35) and AB concentrations (r = 0.27) is observed for out-of-cloud periods. The effect of rain is discussed in the Supplement in Sect. 4.

Only weak correlation were found between AB and ABC concentrations with eBC and NO_x concentrations, suggesting that air pollution has minimal influence on the concentration of these particle types compared to temperature. However, B and BC concentrations show the strongest correlation with eBC mass concentration (0.71 and 0.65, respectively). The correlation increases when using daily means (r = 0.82). Additionally, B and BC concentrations have stronger correlations with NO_x than AB and ABC particles, indicating a greater influence from anthropogenic pollution. This strong correlation between either B or BC concentrations with eBC has been reported a few times in literature (Beck et al., 2024; Markey et al., 2024; Gao et al., 2024; Yue et al., 2022). Therefore, B and BC particles are considered to be mostly of anthropologic origin. See Supplement Sect. 2 for more details of B and BC particles.

To further analyze the relationship between ABC particles and meteorological parameters, data were divided by season, considering only out-of-cloud periods. R.H., temperature and wind speed were binned to channels with widths of 5 %, 2 °C and 2 $m\,s^{-1}$, respectively. Median values of hourly mean concentrations within each bin were calculated, if more than 10 values exist for that bin. In spring and winter, R.H. has little effect on ABC particle concentration, whereas in summer, a linear positive relationship appears, with maximum median concentrations occurring at 80-100 % R.H. (Fig. 6 (a)). A similar but weaker trend is observed in autumn. In spring, summer and autumn, ABC concentrations increase with temperature up to 15 °C but decline at higher temperatures in summer (Fig.6 (b)). Wind speed has the strongest effect in summer, with peak median concentrations on calm days (< 4 ms^{-1}) (Fig. 6 (c)).

Overall, ABC (and AB, data not shown) concentrations peak under high R.H., moderate temperatures (10-15 °C), and low wind speeds in summer. In autumn, higher temperatures and R.H. positively influence ABC concentrations, but low wind
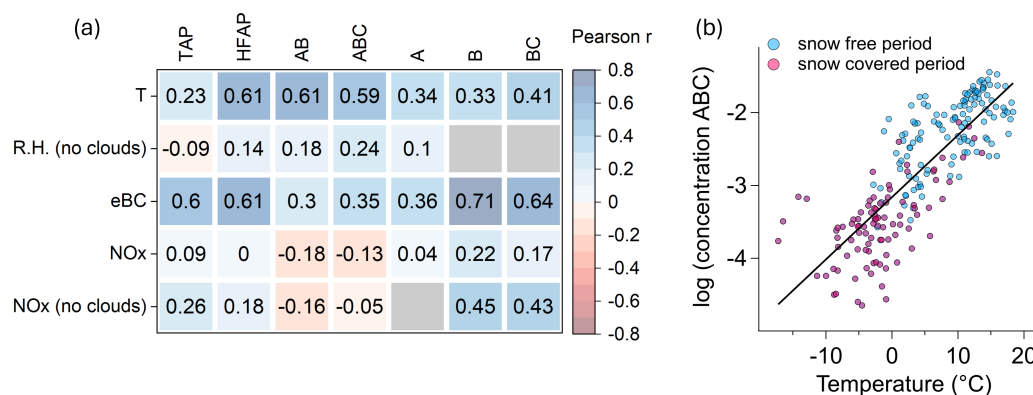
Figure 5. Relation of concentration of particles types to meteorological parameters and air pollution. (a) Pearson correlation coefficient matrix of 1 hour mean values. Grey (empty) relations do not reach the 95 % confidance level. (b) scatter plot of the common logarithm of daily mean ABC particles against ambient temperature (r = 0.82).
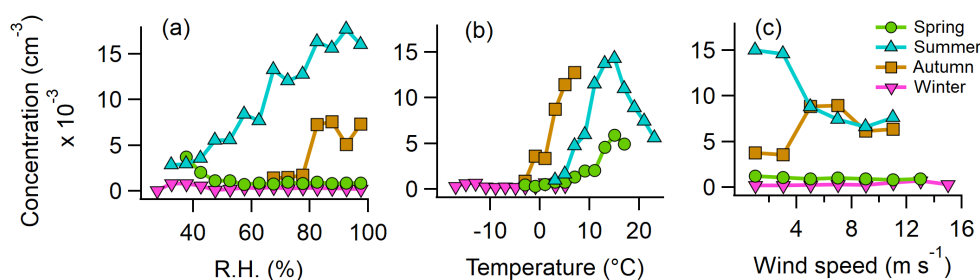
Figure 6. The median concentration of ABC particles dependent on meteorological parameters for each season. Depicted are median concentration values for 1 h mean values. (a) R.H., (b) ambient Temperature, (c) wind speed.

speeds are less favorable. In spring, temperature (up to 15 °C) is the dominant factor, whereas in winter, none of the three

350 meteorological variables have a distinct effect. Similar trends are observed for AB particles, while B and BC particles show no clear relationship to R.H. but increase with temperature in summer and spring.

3.5 ABC particles are dominated by fungal spores

From June 14, 2023, a Burkard trap was installed on the rooftop of Sammaltunturi station to collect airborne pollen grains and fungal spores for microscopic identification. To further differentiate WIBS data and to compare it with Burkard trap

355 measurements, we analyzed the absolute fluorescence intensity in the FL1 channel of each detected ABC particle during the second part of the campaign. We found a multi-modal intensity distribution and identified three distinct fluorescence intensity regions (compare with Clancy et al. (2025), who observed a bimodal distribution). We defined a new FL1 threshold

at 1.0×10^9 intensity units. ABC particles exceeding this new threshold were labeled ABC_3, while all other ABC particles were labeled ABC*. It should be stressed, that the fluorescence threshold used to discriminate ABC* and ABC_3 in this study is not universal and could differ strongly from one individual instrument to another. More details on the trimodal intensity distribution is provided in the Supplement in Sect. 5.

The majority of pollen grains identified in the Burkard trap were pine (*Pinus*, 67 %) and from the cypress familiy (*Cupressaceae*, 12 %) of which most were detected before July. Figure 7 (a, top), shows the total pollen, pine pollen and ABC_3 concentrations, revealing a highly similar timely evolution. A scatter plot of ABC_3 versus pine pollen concentration (Fig. 7 (b, left) shows a strong correlation (r = 0.92, p < 0.0001). Similarly, ABC_3 and total pollen concentration have an r-value of 0.90. The absolute concentrations of both ABC_3 and pine pollen are comparable ($\approx 45°$ linear fit).

Figure 7 (a, bottom), shows identifiable fungal spores and identifiable plant spores from the Burkard trap and ABC* particle concentrations. 90 % of identifiable fungal spores are *Cladosporium*, the remaining 10 % are shared by *Alternaria*, *Pucciniales* (rust fungi) and smut fungi. Identifiable plant spores were 87 % trilete spores, while the rest consists of *Equisetum*, fern and *Lycopodium*. The correlation between fungal spores and ABC* particles is not as pronounced as with pine pollen and ABC_3 particles, but most of the peaks align. The scatter plot of ABC* and spores (fungal spores and plant spores) (7 (b, right), reveals an r-value of 0.65 (p < 0.0001).

Importantly, r-values only change minimally when using all ABC particles instead of ABC* particles, since the concentration of ABC_3 particles is very low compared to ABC*. The sum of ABC* and AB (as well as ABC and AB) leads to similar r-values as ABC* or ABC alone, namely 0.66. This again is an argument for the same nature (of most) of both ABC and AB particles.

Interestingly, ABC_3 and ABC* particles not only differ significantly in the intensity of their fluorescence, but also in size (Fig. 7 (c), left) and in asymmetry factor (Fig. 7 (c), right). The ABC* size distribution peaks at around 3 µm, whereas ABC_3 particles are exclusively found above 2 µm, with a sharp decline after 8 µm, likely due to losses in the inlet system. The asymmetry factor of ABC* particles is low with a maximum of the distribution at 10. Hence, they are relatively sphere-like. The asymmetry factor of ABC_3 particles, on the other hand, is higher with a maximum of the distribution at 50. The differences in fluorescence, size, shape and relation to pollen grains and fungal spores suggest two distinct particle natures.

Despite the high correlation between ABC_3 particles and pollen, it can be ruled out that ABC_3 particles are pollen grains. Pine pollen ranges from 51–100 µm (Halbritter et al., 2021), a size not detected by WIBS. Additionally, the WIBS inlet system significantly loses particles >10 µm (Gratzl et al., 2025). Even if some pine pollen were as small as 10 µm, WIBS would detect only a fraction, contradicting the observed similarity in concentrations. In recent years, the presence of sub-pollen particles in the atmosphere has been studied. These are starch granules which can be expelled from pollen grains during humid conditions and thunderstorms (Burkart et al., 2021) and have been found to fluoresce (partly) in the ABC channel (Hughes et al., 2020; Stone et al., 2021; Mampage et al., 2022). However, they are usually smaller than 2.5 µm in diameter (Burkart et al., 2021; Hughes et al., 2020; Mampage et al., 2022; Suphioglu et al., 1992; Schleh et al., 2010), while ABC_3 particles are larger than 2 µm. A possible explanation could be pollen fragments, as observerd by Hughes et al. (2020), or other plant material that is emitted at the same time as pollen.
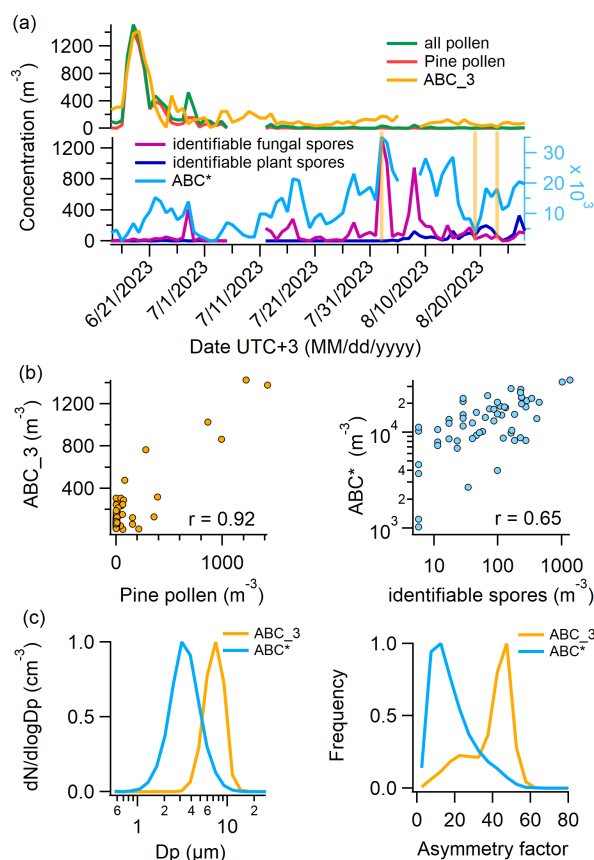
Figure 7. Comparison of Burkard- and WIBS data. (a) top: Daily number concentrations of all pollen, pine pollen (which make up 77 % of all pollen), and ABC_3 particles (ABC particles with FL1 fluorescence intensity $> 1 \times 10^9$ in arbitrary units). (a) bottom: Daily number concentrations of identifiable fungal spores, identifiable plant spores and ABC* particles (all ABC particles without ABC_3 particles). (b) left: Scatter plot of ABC_3 vs. pine pollen concentrations. (b) right: Scatter plot of ABC* vs. identifiable spores concentrations (fungal and plant). (c) left: Normalized size distribution of ABC_3 and ABC* particles. (c) right: Normalized asymmetry factor distribution of ABC_3 and ABC* particles.

Noticeably, the concentration of ABC* particles (and all ABC particles) is much higher than that of identifiable fungal spores with daily averages exceeding spore counts by factors of 20 to 2000. To explain this difference, three days were selected, on
395   which the Burkard data was investigated closer: One of high ABC concentration (August 2, 2023), one of medium ABC concentration (August 23, 2023) and one of low ABC concentration (August 19, 2023) (marked orange on Fig. 7 (a)). For these days, every single particle impacted on the Burkard trap that is definitely or probably a fungal spore (latter contribute between 7 and 13 %), even if it could not be assigned taxonomically, was counted (more than 7000 spores). The resulting daily mean concentration of identifiable fungal spores, total fungal spores (in the Burkard trap), ABC particles as well as AB+ABC
400   for the three days is given in Tab. 1. The concentration of total fungal spores is in the same order of magnitude as the ABC

Table 1. Concentrations of identifiable fungal spores, total fungal spores (counted on the Burkard tape), ABC particles and the sum of AB and ABC particles on three selected days. The concentration differences between identifiable spores and ABC particles are 1, 2 and 3 orders of magnitude. Total spores are in the same order of magnitude as ABC and AB+ABC concentrations.

	August 2, 2023	August 19, 2023	August 23, 2023
identifiable fungal spores (m^{-3})	1339	23	69
total fungal spores (m^{-3})	14466	6132	22119
ABC particles (m^{-3})	35359	4046	18086
AB+ABC particles (m^{-3})	48538	8995	28670

particle concentration, compared to a 1, 2 and 3 orders of magnitude difference between identifiable fungal spores and ABC particles for August 2, 2023, August 19, 2023 and August 23, 2023, respectively. As a result, only a minor fraction of the whole fungal spore population is recorded, when only those fungal spores that can be taxonomically assigned are considered, consistent with Pashley et al. (2012), who found that over 87 % of genera was not identified microscopically). A microscopy
405 picture of the Burkard tape on August 2, 2023 can be seen in the Supplement in Sect. 6. The sum of AB and ABC particles still is considerable higher than that of total fungal spores, especially on August 2. The Burkard trap likely underestimates smaller spores due to strongly increasing difficulties to correctly identify particles as fungal spores, especially colorless (hyaline) ones, with decreasing size. Furthermore, despite being used in aerobiological studies since more than 70 years, to the best knowledge of the authors, a characterization of the detection efficiency of a Hirst type spore trap has never been done for particles < 10 μm.
410 On the other hand, the WIBS (at least in the present study) fails to correctly count the bigger fungal spores due to inlet losses. Surprisingly, both methods give comparable concentration, at least on days with medium and low ABC concentrations. In a similar boreal forest environment Helin et al. (2017) found that airborne fungal DNA was predominantly found in the particle size range < 10 μm, and Abrego et al. (2024) found that the community-weighted mean spore size of continental polar fungal spores is below 5 μm. This highlights the importance of fungal spore measurements in the smaller size range.
415 Most field studies also found that the highest correlation with fungal spores was achieved with ABC particles (Sarangi et al., 2022; Fernández-Rodríguez et al., 2018). Similar results were found when comparing WIBS data with fungal spore tracers (Yue et al., 2019, 2022; Gosselin et al., 2016). In chamber studies, however, fungal spores have been characterized almost exclusively as A particles (Hernandez et al., 2016; Savage et al., 2017). In our study, A particles showed no significant correlation to identifiable fungal spore counts (differing to Markey et al. (2022)). This discrepancy could have two main reasons. (a):
420 Atmospheric aging (e.g., UV radiation, water uptake, other atmospheric components (Pan et al., 2021)) may alter fluorescence properties. For instance, fluorescence of *Aspergillus niger*, a common mold fungus, was strongly enhanced after UV-light exposure (Raimondi et al., 2009). This could lead to stronger fluorescence in the FL3 channel for air-exposed fungal spores compared to laboratory grown cultures and therefore to an enhanced ABC signal. (b): There could be significant instrument variability of obtained fluorescence signals (Hernandez et al., 2016), which might even be enhanced when comparing different
425 model versions of the WIBS.

Some studies report poor correlation between WIBS data and *Cladosporium* counts (Healy et al., 2014; O'Connor et al., 2015), possibly due to the fact that *Cladosporium* spores can get released in larger clusters which either get counted as one single particle by the WIBS or is lost in the inlet (Markey et al., 2022). However, in this study, *Cladosporium* spores dominate identifiable fungal spores and drive peak ABC* concentrations (Fig. 7 (a, bottom)). Subtracting *Cladosporium* counts reduces

430 the correlation (r = 0.39, p < 0.05), suggesting clustering issues may be less significant at our high-altitude site with sparse vegetation. In summary, WIBS data suggest that most ABC particles correspond to fungal spores, although pollen fragments or other plant material may also contribute.

3.6 DNA analysis reveals dominance of Basidiomycota in air samples

To gain a deeper understanding of fungal spore diversity beyond the identifiable (mostly) Ascomycota observed in Burkard

435 slides, we collected 8 bi-daily air filters from September 16 to 19, 2023, extracted DNA, performed fungal barcode sequencing and taxanomic assignment. Parallel impactor measurements and microscopic analysis indicate that the majority of particles with Da > 1 μm during this time are likely fungal spores (see Fig. 8 for a representative example). Figure 9 displays boxplots showing the contributions of Basidiomycota and Ascomycota to the total fungal reads, revealing that the vast majority of fungal DNA originated from Basidiomycota (median value: 90.1 %). In contrast, the identifiable fungal counts from the Burkard data

440 showed approximately 90 % Ascomycota, suggesting that the majority of unidentifiable spore counts in the Burkard data are Basidiomycota. The median contribution of Ascoymocota from the sequencing data is 8.8 %. Noticeably, 2 data points stand out: There was a snowstorm during loading of the last 2 filters (red dots in Fig. 9). For these data points, fluorescent particle concentrations (see Supplement Sect. 8) and read numbers from high-throughput sequencing were much lower. The latter is indicative of low DNA concentrations in the starting material due to low spore numbers on filters. Consequently, the absolute

445 abundance of Ascomycota is still much lower than on the other sampling days. Within the Basidiomycota, a majority of spores belong to the Agaricomycetes (median value: 99.6 %), including the 14 most abundant fungi. This finding aligns with previous studies by Maki et al. (2023); Fröhlich-Nowoisky et al. (2012); Yamamoto et al. (2012) and Fröhlich-Nowoisky et al. (2009) which reported that Agaricomycetes dominate airborne Basidiomycota and are among the most abundant atmospheric fungi. Notably, none of the Agaricomycetes identified through DNA analysis could be visually identified. Within the Agaricomycetes,

450 the most abundant fungi belong to the order Agaricales (median: 48.7 %), Atheliales (8.0 %), Russales (4.4 %) and Polyporales (4.1 %).

Although the two methods were not used simultaneously (with a two-day gap), we compare Burkard data from shortly before the DNA sampling period (September 11 to 13, 2023) with the three days of DNA sampling under similar, although colder weather conditions (September 16 to 18, 2023). During the relevant days, 100 % of identifiable fungal spores from the Burkard

455 data were *Cladosporium* with a mean concentration of 30.5 m^{-3}. eDNA analysis reveals, that only 0.44 % of all fungal reads is from *Cladosporium*. Extrapolating from the difference of *Cladosporium* counts and reads to 100 % gives an estimated total spore concentration of 6932 spores m^{-3}, which agrees with the concentration of fluorescent particles > 1 μm (Da) measured with the impactor and fluorescence microscope within one order of magnitude (3010 m^{-3}; see Supplement Sect. 8 for more details).
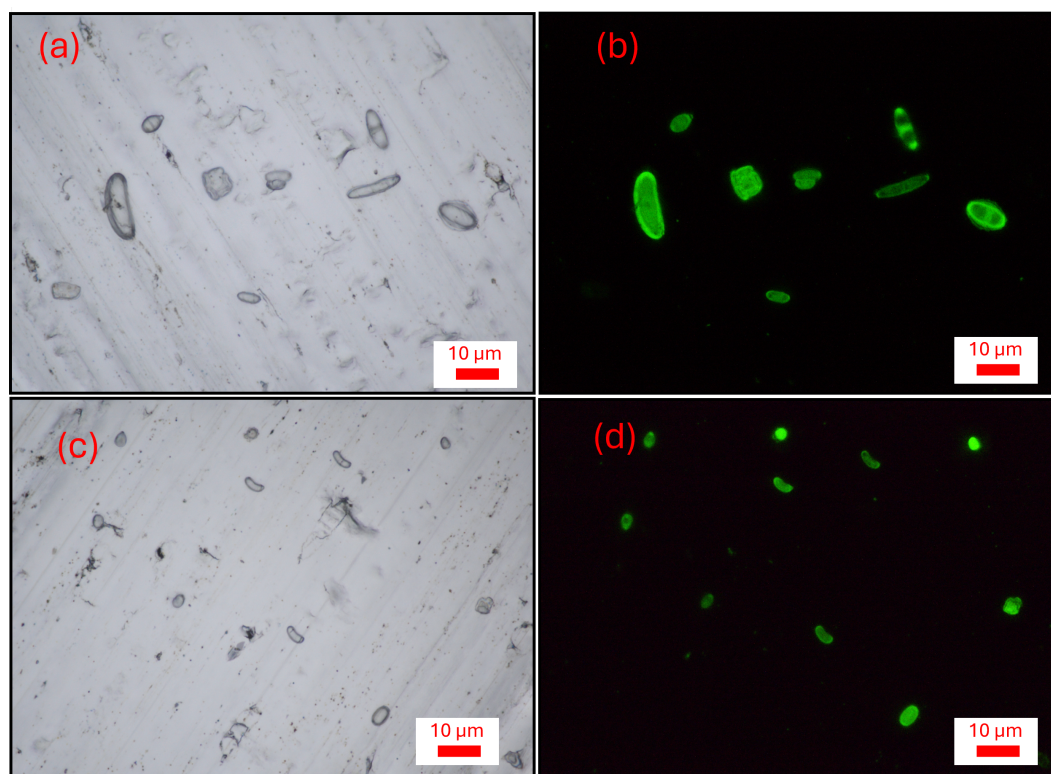
Figure 8. Representative examples of fluorescence and light microscopy pictures of impactor samples from September 19, 2023 9 am - 4 pm. (a) Particles from stage A (Da > 2.5 µm), (b) Same as (a) but only fluorescent particles. (c) Particles from stage B (1.0 < Da < 2.5 µm), (d) same as (c) but only fluorescent particles. Most particles show strong fluorescence and have a characteristic shape.

460   A large fraction of Basidiomycota uses a passive spore discharge mechanism (surface tension catapult) (Elbert et al., 2007; Pringle et al., 2005), where a drop and a film of water has to condensate on the spores in order to get expelled in the air (called ballistospores) (Zoberi, 1964). Consequently, most Basidiomycota prefer high R.H. and moderate temperatures for spore release (Fröhlich-Nowoisky et al., 2016; Gilbert and Reynolds, 2005; De Groot, 1968). Ballistospores from Basidiomycota typically range from 2 to 10 µm in diameter (Elbert et al. (2007) and references therein). As we have mostly detected reads

465   from Basidiomycota (Fig. 9) and most of the particles we analyzed under the microscope are likely fungal spores (Fig. 8), this indicates that most fungal spores detected were basidiospores. As shown in Fig. 6 (a), the concentration of ABC particles in summer (and to a lesser extent in autumn) is strongly influenced by ambient relative humidity and moderate temperatures (approximately 15 °C being most favorable). Additionally, ABC particles predominantly range between 1 and 10 μm in diameter (Fig. 10 (c)), further supporting our argument that ABC particles are primarily fungal spores of Basidiomycota.
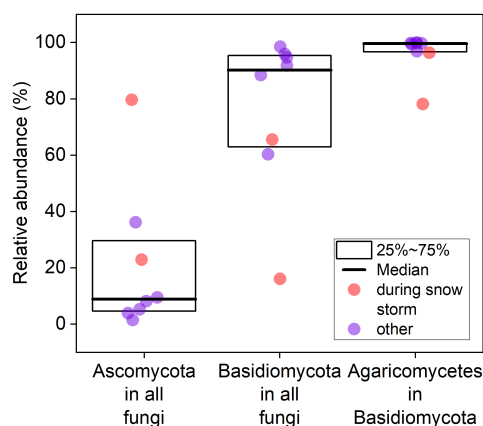
Figure 9. Relative abundance of Ascomycota, Basidiomycota and Agaricomycetes in Basidiomycota based on fungal reads. Data was collected from 8 individual filters.

3.7 Fungal spores are highly active INPs

We compared the concentration of ABC particles (and all other HFAP types) to INP concentrations over a wide range of temperature, incorporating data from PINE during the PaCe22 campaign as well as filters for INSEKT, both collected in parallel to WIBS data. For correlation analysis, PINE data was averaged to 1 hour. Filters for INSEKT analysis were changed weekly, with exception for 6 bi-daily filters at the beginning and 8 bi-daily filters at the end of the second part of the campaign. The bi-daily filters were averaged for consistency with weekly filters. Figure 10 (a) shows the time series of INPs active at -13.5 °C ($N_{\mathrm{INP}}(-13.5)$) alongside ABC concentrations scaled by 0.0022 for comparison. The lowest detectable INP concentration $9 \times 10^{-4}\,\mathrm{l}^{-1}$ was recorded in early May, while the highest concentration ($0.085\,\mathrm{l}^{-1}$) occurred on the second week of August. Despite data points of INPs and ABC particles spanning over two orders of magnitude, all peaks and valleys compare very well. In fact, the INP-to-ABC ratio (multiplied by 0.0022) mostly remains near 1. Therefore, approximately 0.22 % of ABC particles are responsible for the INP concentration at this temperature and the contribution of ABC particles to INPs is relatively constant over the whole period. Thus, practically all INPs active at this temperature are ABC particles, and therefore probably fungal spores.

The relation between $N_{\mathrm{INP}}(-13.5)$ and ABC data show the highest correlation of any WIBS-INP comparison, namely r = 0.94 (p< 0.0001) (Fig. 10 (b), marked with dashed line). In general, ABC particles gave the highest correlation coefficient for almost all temperatures. In (Fig. 10 (b)), the Pearson correlation coefficient for the INP-ABC correlation at all temperatures that reach a confidence level of 95 % are plotted. Between -12 °C and -15 °C, all Pearson values are above 0.8 (with highest p value of 1.2×10^{-5}). Hence, they are very likely to be composed of ABC particles and are therefore of fungal origin. Since AB
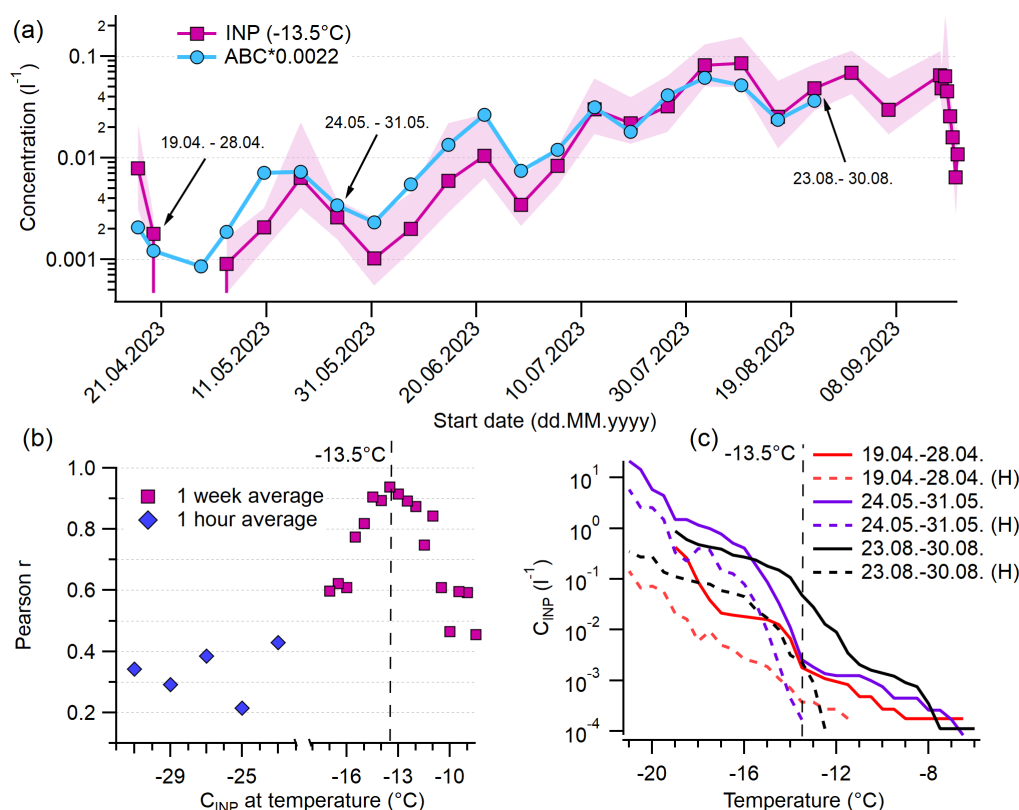
Figure 10. Relation of ABC particles to INPs. (a) Concentrations of weakly INPs active at -13.5 °C and ABC concentration multiplied by 0.0022. (b) Pearson correlation coefficient of correlation of ABC particles with INPs active at certain temperature. (c) Cumulative INP spectra of 3 selected days (also marked in (a)) and spectra of the same day with prior heat treatment (H).

and ABC likely share a biological source, their combined correlation was tested but showed little difference from ABC alone. At both warmer and colder temperatures, INP-ABC correlations weaken. Above -10 °C, bacteria could play an important role

490 in heterogeneous ice nucleation (Kanji et al., 2017; Šantl Temkiv et al., 2015; Morris et al., 2004; Jayaweera and Flanagan, 1982), yet they are unlikely captured in the ABC channel of the WIBS (Hernandez et al., 2016; Savage et al., 2017), but in the A channel. However, we did not find a correlation of A particles within a confidence level of 95 % for temperatures > -8.5 °C. For the whole temperature regime covered with INSEKT, only for one temperature (-10°C), a significant correlation with TAPs ($r = 0.60$, $p < 0.005$) was found, although, since all neighboring temperatures do not show a significant correlation, this

495 finding should be treated with caution.

Below -15 °C, biological particles might not be the dominating source of INPs, as mineral dust, inorganic particles, and combustion aerosols also nucleate ice (DeMott and Prenni, 2010; Murray et al., 2012; Kanji et al., 2017). Pearson r-values for 1 hour mean ABC and PINE data (Fig. 10 (b)) range between 0.43 (-22 °C) and 0.22 (-25 °C). AB+ABC particles had

slightly higher correlations than ABC alone. r-values for HFAPs range from 0.32 to 0.47. As HFAPs most likely consist of
both biological and other particles (see Supplement Sect. 2), the significance of biological aerosols for INPs active at colder
temperatures can not be clarified. The lowest Pearson r-values for the temperatures -23 °C, -25 °C and -27 °C all belong to
TAPs and are below 0.28.

For selected samples, a heat treatment with a subsequent INP analysis was performed. INP concentrations before and after
heat treatment are shown for three representative filters (April, during snow cover; May, shortly after snow melt; August),
marked with arrows in Figure 10 (a). After heat treatment, the vast majority of INPs active at -13.5 °C (marked with vertical
dashed line) vanishes. This is typically associated with the presence of biological proteinaceous INPs whose ice nucleation
ability is sensitive to heat (Daily et al., 2022; Huang et al., 2021; Šantl Temkiv et al., 2019).

Direct comparisons between INPs and bioaerosols in field studies have grown with the adoption of LiF sensors in atmo-
spheric science. Similar findings have been reported in a range of natural environments. For instance, Schneider et al. (2021)
found that ABC particles correlated best with INPs active at -16 °C in a boreal forest (Hyytiälä). Tobo et al. (2013) reported
a significant correlation (r = 0.78, p < 0.01) between INPs at -15 °C and fluorescent aerosol particles (FAPs) in a Colorado
Pine forest using a UV-APS in summer . Similar results were obtained by Prenni et al. (2013); Wright et al. (2014); Mason
et al. (2015); Twohy et al. (2016); Cornwell et al. (2023); Kawana et al. (2024) and Taketani et al. (2025). However, these
studies were not able to pinpoint the nature of the fluorescent particles. Pereira Freitas et al. (2023), combined FAP data us-
ing the multiparameter bioaerosol spectrometer (MBS, University of Hertfordshire, UK) with offline measurements of fungal
spore tracers in Ny-Ålesund, Svalbad. The authors also found a high correlation of $N_{\mathrm{INP}}(-15)$ and FAPs. Additionally, the
fungal spore tracers imply that the terrestrial biosphere, and potentially fungal spores are an important contributor to the INP
population during arctic summer after snow melt. Size resolved measurements of INPs confirm that most INPs active at -15 °C
exceed 1 µm (Da), with 70 % > 2.5 µm in the arctic (Mason et al., 2016). This aligns with earlier studies (Mason et al., 2015;
Huffman et al., 2013) which additionally found PBAPs in a similar size range, of which a majority showed typical features of
fungal spores. This is in agreement with the size distribution of ABC particles measured here (Fig. 7 (c) left): The majority of
ABC particles is bigger than 2.5 μm, and almost no particles < 1 μm were detected.

The relationship between PBAPs and colder temperature INPs (< -22 °C) remains unclear. Similar correlation coefficients of
those obtained here, were reported by Vogel et al. (2024) in Hyytiälä between mid-March and mid-May. In contrast Paramonov
et al. (2020) found no significant correlation of fluorescent particles with colder temperature INPs, during March and April
at the same location, and Lacher et al. (2021) reported that while FAPs correlated with INPs at Jungfraujoch (3571 m above
sea level), TAPs showed an even higher correlation. In both cases, snow-covered ground likely suppressed local biogenic
aerosol emissions. Gao et al. (2024), on the other hand, reported, that PBAPs play a major role at Mount Helmos in the eastern
Mediterranean over wide range of activation temperatures, including < -20 °C.

3.8 The ice nucleation ability of detected fungal spores

In this study, we presented a comprehensive dataset of HFAPs and demonstrated, through comparisons with fungal spore counts
and eDNA analysis, that the vast majority of INPs active above -15 °C are most likely fungal spores. However, as previously

discussed, fungal INA has been studied much less than for example pollen INA. This is mainly due to the immense diversity of fungi (estimated at 2.2 to 5.1 million species) of which only a fraction has been discovered or described (Hawksworth and
535 Lücking, 2017; Blackwell, 2011).

Among the fungi identified at least to the genus level via eDNA analysis (154 unique genera), species from 6 genera have previously been tested for ice nucleation. Table 2 lists these detected genera alongside the activation temperatures of specific species tested, the species identified in this study, and their mean relative abundance across the four measurement days (eight filter samples).

540 Not all species within a genus exhibit ice nucleation. Most tested species show very low or no ice nucleation temperature in immersion mode freezing (including all tested species of *Aspergillus*, *Trichaptum* and *Trichoderma*). Within the *Cladosporium* genus, only *C. herbarum* showed ice nucleation at -15 °C (Jayaweera and Flanagan, 1982), though this result was not confirmed by Pummer et al. (2013), likely due to differences in freezing volume (Wieland et al., 2025) or cultivation conditions (Pummer et al., 2013; Tsumuki et al., 1995). The species detected here (*C. cladosoroides*) was found to not nucleate ice (Pummer et al.,
545 2013)). Given that *Cladosporium* counts from the Burkard trap alone should be sufficient to explain INP concentrations, it is unlikely that *Cladosporium* is responsible for the high-temperature INPs observed here. Conflicting results also exist for *Penicillium digitatum* which has been reported to nucleate ice at both -10 °C (Jayaweera and Flanagan, 1982) and -33 °C (Pummer et al., 2013). All other tested *Penicillium* species have activation temperatures of -22 °C or lower. In this study, we detected 4 species of *Penicillium* (each on one filter only) of which non has been tested for INA. The most ice active fungus
550 known today is *Fusarium*, with a nucleation temperature around -5 °C (Kunert et al., 2019; Pummer et al., 2013; Pouleur et al., 1992). One of the four species detected here, (*F. tricinctum*) nucleates ice at -7.3 °C (Kunert et al., 2019). However, it was only detected on 1 out of the 8 filters. two other detected species (*F. equiseti*, *F. oxysporum*) show no INA (Kunert et al., 2019; Pummer et al., 2013) and the third (*F. solani*) has not yet been tested. *Fusarium* was never detected with the Burkard trap. Thus, it remains unclear whether *Fusarium* and *Penicillium* contributes significantly to high temperature ice nucleation.
555 The most abundant class of fungi here are the Agaricomycetes. Some species of this class which were not detected here, have been tested for INA in laboratory studies by Haga et al. (2014) and Pummer et al. (2013) and revealed very low or no ice nucleation. However, none of the 84 unique genera of Agaricomycetes detected in this study have been tested for INA. Recent field studies suggest that Agaricomycetes may contribute to atmospheric high temperature ice nucleation (Tang et al., 2022). Specifically *Hypholoma*, one the most abundant fungi here (median relative abundance of 3.4 % (mean: 4.3 %)) as well as
560 *Sistotrema* (median: 1.1 % (mean: 5.3 %)), have been proposed as high temperature ice nuclei, based on comparison of relative atmospheric abundance and INP concentrations (Niu et al., 2024).

4 Conclusions

This study presents size-resolved measurements of HFAPs over 4 season in the Finnish sub-Arctic, demonstrating that AB and ABC particles dominate the HFAP fraction during warmer periods. Meteorological conditions, particularly snow cover,
565 significantly influence AB and ABC particle concentrations. Snow cover led to an immediate reduction in these particle types,

Table 2. Ice nucleation temperatures (immersion freezing) of species whose genus was detected via eDNA analysis on filter samples and the detected species and its mean relative abundance. The number in brackets refers to the number of filters the species was detected on (out of 8 filters) T_{50} and T_{96} are the temperatures at which 50 % and 96 % of sample containing droplets froze, respectively, and T_{onset} is the temperature at which the first droplet froze. Species in bold letters are the only species detected, which have been tested for INA before. *sp.* means that different species of the genus are grouped together because they cannot be resolved more precisely.

Genus	Species detected	mean abundance (%)	Species	INA (°C)	Reference
Cladosporium	**C. cladosoroides**	0.40 (5)	**C. cladosoroides**	no INA	(Pummer et al., 2013), T_{50}
			C. herbarum	no INA	
			C. herbarum	-15	(Jayaweera and Flanagan, 1982), T_{96}
			C. sp.	-35.1	(Iannone et al., 2011), T_{50}
Penicillium	*P. bialowiezense*	0.15 (1)	*P. notatum*	-22	
	P. melinii	0.08 (1)	*P. frequentes*	-22	(Jayaweera and Flanagan, 1982), T_{96}
	P. rubens	0.04 (1)	*P. digitatum*	-10	
	P. rubens	0.04 (1)	*P. digitatum*	-33	(Pummer et al., 2013), T_{50}
			P. chrysogenum	no INA	
			P. citrinum	no INA	
			P. glabrum	no INA	
			P. sp	-27	(Haga et al., 2014), T_{onset}
			P. brevicompactum	-27	
Aspergillus	*A. penicillioides*	0.33 (4)	*A. brasiliensis*	-25	
	A. tardicrescens	0.02 (1)	*A. niger*	-29	(Pummer et al., 2013), T_{50}
			A. niger	no INA	
			A. fumigatus	-34	
			A. oryzae	-31	
Fusarium	**F. tricinctum**	0.13 (1)	**F. tricinctum**	-7.3	(Kunert et al., 2019), T_{50}
	F. equiseti	3.8 (3)	**F. equiseti**	no INA	
	F. oxysporum	0.04 (1)	**F. oxysporum**	no INA	
	F. solani	0.02 (1)	**F. oxysporum**	no INA	(Pummer et al., 2013), T_{50}
			F. acuminatum	-3.5 to -6.3	(Kunert et al., 2019), T_{50}
			F. acuminatum	-5	(Pouleur et al., 1992), T_{onset}
			F. avenaceum	-2.5	
			F. avenaceum	-9	(Pummer et al., 2013), T_{50}
			F. avenaceum	-5.0 to -7.6	(Kunert et al., 2019), T_{50}
			F. armeniacum	-5.3	
			F. begoniae	-11.2	
			F. concenticum	-4.6	
			F. langsethiae	-7.3	
Trichaptum	*T. fuscoviolaceum*	0.13 (2)	*T. abietnium*	-26	(Haga et al., 2014), T_{onset}
Trichoderma	*T. rossicum*	0.04 (1)	*T. atroviride*	-32 to -35	(Pummer et al., 2013), T_{50}
	T. aeroaquaticum	0.02 (1)	*T. longibrachiatum*	-32	
	T. harzianum	0.02 (1)	*T. reesei*	no INA	
			T. virens	no INA	

suggesting that as soon as the local biosphere is (partially) buried under a thick layer of snow, the emission of PBAPs is reduced strongly. Diurnal pattern confirmed the local origin of the PBAPs, as concentrations where highest when the station was inside the mixing layer, and therefore coupled to the local surface. A comparison with direct fungal spore and pollen counts confirmed that ABC particles predominantly consist of fungal spores, and a newly applied fluorescence threshold strategy

570   revealed that a minor fraction of ABC particles correlated with pollen grains. Visual identification of fungal spores using the Burkard trap is limited to a taxonomic group where reliable recognition is possible, and accounted for only a fraction (3–10 %) of total fungal spores. This finding was supported by eDNA analysis, which showed that most fungal genera detected belong to Basidiomycota, particularly Agaricomycetes, of which none could be visually identified as such. A strong correlation between ABC particle concentrations and high-temperature INPs suggests that fungal spores are the dominant INPs active at tempera-

575   tures around -13.5 °C. However, eDNA analysis did not pinpoint specific ice-nucleating fungal species, as only a small subset of fungal genera has been tested for ice nucleation activity, and activation temperatures above -15 °C are rare among tested genera. This leaves an open question regarding the exact biological particles responsible for high-temperature ice nucleation. Despite this uncertainty, our study marks a significant step in demonstrating that fungal spores, likely originating from the local biosphere, dominate the INP population active above -15 °C. Further testing of Agaricomycetes for INA is needed to

580   determine which specific species or genera contribute to atmospheric ice nucleation. However, Basidiomycota (which include Agaricomycetes) are generally more difficult to cultivate than Ascomycota (Rungjindamai and Jones, 2024; Krupodorova et al., 2021). Additionally, cultivation conditions and strain selection can influence INA (Pummer et al., 2013; Tsumuki et al., 1995), posing a significant challenge for future research.

The fungal fruiting season is expected to lengthen due to climate change (Boddy et al., 2014), and the fungal spore season

585   is advancing (Wu et al., 2024). Simultaneously, the snow-covered period in the subarctic is projected to shorten (Dankers and Christensen, 2005). These changes suggest that fungal ice nucleation in Arctic and sub-Arctic regions may become increasingly significant, as ice-active fungal spores could remain available over a longer portion of the year. Future climate models should account for these shifts to better understand the impact of fungal high-temperature INPs on low-level cloud feedback at high latitudes.

590   *Data availability.* WIBS data from the PaCE22 campaign is available at the open data repository Zenodo under the doi 10.5281/zenodo.13885888 (Gratzl, 2024). A data description paper is provided by Gratzl et al. (2025).

WIBS data from the second part of the campaign and relative contributions of fungal species via eDNA analysis is available at the open data repository TU Wien Research Data under the doi 10.48436/0xmsb-eps20 (Gratzl and Grothe, 2025).

PINE data from the PaCE22 campaign is available at the open data repository Zenodo under the doi 10.5281/zenodo.13889647 (Böhm-

595   länder et al., 2024). A data description paper is provided by Böhmländer et al. (2025).

INSEKT data will be available at the an open data repository before the manuscript is accepted.

Burkard data will be available in the context of the SYLVA (A SYstem for ReaL-Time ObserVation of Aeroallergens) project in near future or upon request.

Meteorological data, eBC, SO$_2$ and NOx concentrations are available at https://en.ilmatieteenlaitos.fi/download-observations (last access:
600 26.02.2025) for the observation station "Muonio Sammaltunturi".

Author contributions. J.G., A.B., D.B., K.D., E.A., O.M. and H.G. conceived and planned the experiments. D.B. and K.D. prepared and organized the PaCE 2022 campaign. J.G. performed WIBS measurements and data analysis, analyzed impactor foils with fluorescence microscopy, combined and interpreted all data with contributions from all authors, visualized data. J.G., F.W., and O.M. collected filter samples. A.B. performed PINE and INSEKT measurements and analyzed data. S.P. and C.P. performed pollen and spore counts and analyzed
605 data. C.P. and M.G. performed the eDNA measurements and analyzed data. J.G. wrote the manuscript with support from A.B., S.P., C.P., M.G., K.D. and E.A. All authors discussed the results and reviewed and edited the manuscript.

Competing interests. At least one of the (co-)authors is a member of the editorial board of Atmospheric Chemistry and Physics.

Acknowledgements. This work was supported by atmo access under the ID ATMO-TNA-4-0000000069. We gratefully acknowledge support by the FFG (Austrian Research Promotion Agency) for funding under project no. 888109, the Vienna Science and Technology Fund
610 (WWTF) through project VRG22-003, and the Research Council of Finland for ACCC Flagship (project no 359342). The authors gratefully acknowledge the NOAA Air Resources Laboratory (ARL) for the provision of the HYSPLIT transport and dispersion model and/or READY website (https://www.ready.noaa.gov) used in this publication. We thank TU Wien and BMBWF for the purchase of the WIBS 5/NEO. The authors would like to thank the team from Metsähallitus and Sammaltunturi station for their help with logistics, filter changing and watch over our instrumentation. The authors acknowledge the TU Wien Bibliothek for financial support through its Open Access Funding Program.
615 We are also grateful to Anne Kasper-Giebl from TU Wien and Paul Winkler from the University of Vienna for the equipment they lent us. We thank Tobias Könemann from Droplet Measurement Technologies for his technical support. We thank Harald Berger (Symbiocyte, Vienna, Austria) who did the initial bioinformatics. We also like to thank Evgeny Kadantsev from FMI for the fruitfull dicussions.

References

Aalto, T., Hatakka, J., Paatero, J., Tuovinen, J.-P., Aurela, M., Laurila, T., Holmén, K., Trivett, N., and Viisanen, Y.: Tropospheric carbon dioxide concentrations at a northern boreal site in Finland: basic variations and source areas, Tellus B: Chem Phys Meteorol, 54, 110–126, https://doi.org/10.3402/tellusb.v54i2.16652, 2002.

Abarenkov, K., Zirk, A., Piirmann, T., Põhönen, R., Ivanov, F., Nilsson, R. H., and Kõljalg, U.: Full UNITE+INSD dataset for eukaryotes, https://doi.org/10.15156/BIO/2959331, 2024.

Abrego, N., Furneaux, B., Hardwick, B., Somervuo, P., Palorinne, I., Aguilar-Trigueros, C. A., Andrew, N. R., Babiy, U. V, Bao, T., Bazzano, G., Bondarchuk, S. N., Bonebrake, T. C., Brennan, G. L., Bret-Harte, S., Bässler, C., Cagnolo, L., Cameron, E. K., Chapurlat, E., Creer, S., D'Acqui, L. P., de Vere, N., Desprez-Loustau, M.-L., Dongmo, M. A. K., Jacobsen, I. B. D., Fisher, B. L., Flores de Jesus, M., Gilbert, G. S., Griffith, G. W., Gritsuk, A. A., Gross, A., Grudd, H., Halme, P., Hanna, R., Hansen, J., Hansen, L. H., Hegbe, A. D. M. T., Hill, S., Hogg, I. D., Hultman, J., Hyde, K. D., Hynson, N. A., Ivanova, N., Karisto, P., Kerdraon, D., Knorre, A., Krisai-Greilhuber, I., Kurhinen, J., Kuzmina, M., Lecomte, N., Lecomte, E., Loaiza, V., Lundin, E., Meire, A., Mešić, A., Miettinen, O., Monkhouse, N., Mortimer, P., Müller, J., Nilsson, R. H., Nonti, P. Y. C., Nordén, J., Nordén, B., Norros, V., Paz, C., Pellikka, P., Pereira, D., Petch, G., Pitkänen, J.-M., Popa, F., Potter, C., Purhonen, J., Pätsi, S., Rafiq, A., Raharinjanahary, D., Rakos, N., Rathnayaka, A. R., Raundrup, K., Rebriev, Y. A., Rikkinen, J., Rogers, H. M. K., Rogovsky, A., Rozhkov, Y., Runnel, K., Saarto, A., Savchenko, A., Schlegel, M., Schmidt, N. M., Seibold, S., Skjøth, C., Stengel, E., Sutyrina, S. V., Syvänperä, I., Tedersoo, L., Timm, J., Tipton, L., Toju, H., Uscka-Perzanowska, M., van der Bank, M., van der Bank, F. H., Vandenbrink, B., Ventura, S., Vignisson, S. R., Wang, X., Weisser, W. W., Wijesinghe, S. N., Wright, S. J., Yang, C., Yorou, N. S., Young, A., Yu, D. W., Zakharov, E. V., Hebert, P. D. N., Roslin, T., and Ovaskainen, O.: Airborne DNA reveals predictable spatial and seasonal dynamics of fungi, Nature, 631, 835–842, https://doi.org/10.1038/s41586-024-07658-9, 2024.

Agresti, A. and Coull, B. A.: Approximate is Better than "Exact" for Interval Estimation of Binomial Proportions, The American Statistician, 52, 119–126, https://doi.org/10.1080/00031305.1998.10480550, 1998.

Augustin, S., Wex, H., Niedermeier, D., Pummer, B., Grothe, H., Hartmann, S., Tomsche, L., Clauss, T., Voigtländer, J., Ignatius, K., and Stratmann, F.: Immersion freezing of birch pollen washing water, Atmospheric Chemistry and Physics, 13, 10 989–11 003, https://doi.org/10.5194/acp-13-10989-2013, 2013.

Backman, J. e. a.: In-situ aerosol measurement during PaCE 2022, in preparation for Earth Syst Sci Data, 2025.

Barnet, D.: david-barnett/microViz: microViz 0.12.6, https://github.com/david-barnett/microViz, gitHub repository, 2024.

Barry, K. R., Hill, T. C. J., Kreidenweis, S. M., DeMott, P. J., Tobo, Y., and Creamean, J. M.: Bioaerosols as indicators of central Arctic ice nucleating particle sources, EGUsphere, 2025, 1–26, https://doi.org/10.5194/egusphere-2025-128, 2025.

Bauer, H., Claeys, M., Vermeylen, R., Schueller, E., Weinke, G., Berger, A., and Puxbaum, H.: Arabitol and mannitol as tracers for the quantification of airborne fungal spores, Atmospheric Environment, 42, 588–593, https://doi.org/10.1016/j.atmosenv.2007.10.013, 2008.

Beck, H. E., Zimmermann, N. E., McVicar, T. R., Vergopolan, N., Berg, A., and Wood, E. F.: Present and future Köppen-Geiger climate classification maps at 1-km resolution, Scientific Data, 5, 180 214, https://doi.org/10.1038/sdata.2018.214, 2018.

Beck, I., Moallemi, A., Heutte, B., Pernov, J. B., Bergner, N., Rolo, M., Quéléver, L. L. J., Laurila, T., Boyer, M., Jokinen, T., Angot, H., Hoppe, C. J. M., Müller, O., Creamean, J., Frey, M. M., Freitas, G., Zinke, J., Salter, M., Zieger, P., Mirrielees, J. A., Kempf, H. E., Ault, A. P., Pratt, K. A., Gysel-Beer, M., Henning, S., Tatzelt, C., and Schmale, J.: Characteristics and sources of fluorescent aerosols in the central Arctic Ocean, Elementa-Sci Antrop, 12, 00 125, https://doi.org/10.1525/elementa.2023.00125, 2024.

Berner, L. T., Massey, R., Jantz, P., Forbes, B. C., Macias-Fauria, M., Myers-Smith, I., Kumpula, T., Gauthier, G., Andreu-Hayles, L., Gaglioti, B. V., Burns, P., Zetterberg, P., D'Arrigo, R., and Goetz, S. J.: Summer warming explains widespread but not uniform greening in the Arctic tundra biome, Nat Commun, 11, 4621, https://doi.org/10.1038/s41467-020-18479-5, 2020.

Blackwell, M.: The Fungi: 1, 2, 3 ... 5.1 million species?, American Journal of Botany, 98, 426–438, https://doi.org/10.3732/ajb.1000298, 2011.

Boddy, L., Büntgen, U., Egli, S., Gange, A. C., Heegaard, E., Kirk, P. M., Mohammad, A., and Kauserud, H.: Climate variation effects on fungal fruiting, Fungal Ecology, 10, 20–33, https://doi.org/10.1016/j.funeco.2013.10.006, fungi in a changing world: The role of fungi in ecosystem response to global change, 2014.

Böhmländer, A., Lacher, L., Fösig, R., Büttner, N., Nadolny, J., Brus, D., Doulgeris, K.-M., and Möhler, O.: Measurement of the ice-nucleating particle concentration with the Portable Ice Nucleation Experiment during the Pallas Cloud Experiment 2022, Earth Syst Sci Data Discuss, 2025, 1–10, https://doi.org/10.5194/essd-2025-89, 2025.

Böhmländer, A. J., Lacher, L., Brus, D., Doulgeris, K.-M., Brasseur, Z., Boyer, M., Kuula, J., Leisner, T., and Möhler, O.: A novel aerosol filter sampler for measuring the vertical distribution of ice-nucleating particles via fixed-wing uncrewed aerial vehicles, Atmospheric Measurement Techniques Discussions, 2024, 1–22, https://doi.org/10.5194/amt-2024-120, 2024.

Bolger, A. M., Lohse, M., and Usadel, B.: Trimmomatic: a flexible trimmer for Illumina sequence data, Bioinformatics, 30, 2114–2120, https://doi.org/10.1093/bioinformatics/btu170, 2014.

Brus, D., Doulgeris, K., Bagher, G., Bodenschatz, E., Chávez-Medina, V., Pohorsky, R., Schmale, J., Lonardi, M., Favre, L., Böhmländer, A., Möhler, O., Lacher, L., Girdwood, J., Gratzl, J., Grothe, H., Kaikkonen, V., O'Connor, E., Le, V., Backman, J., and Servomaa, H.: Data generated during the Pallas Cloud Experiment 2022 campaign: an introduction and overview, in preparation for Earth Syst Sci Data, 2025.

Burkart, J., Gratzl, J., Seifried, T. M., Bieber, P., and Grothe, H.: Isolation of subpollen particles (SPPs) of birch: SPPs are potential carriers of ice nucleating macromolecules, Biogeosciences, 18, 5751–5765, https://doi.org/10.5194/bg-18-5751-2021, 2021.

Burrows, S. M., McCluskey, C. S., Cornwell, G., Steinke, I., Zhang, K., Zhao, B., Zawadowicz, M., Raman, A., Kulkarni, G., China, S., Zelenyuk, A., and DeMott, P. J.: Ice-Nucleating Particles That Impact Clouds and Climate: Observational and Modeling Research Needs, Reviews of Geophysics, 60, e2021RG000 745, https://doi.org/10.1029/2021RG000745, e2021RG000745 2021RG000745, 2022.

Böhmländer, A., Lacher, L., and Möhler, O.: Data from Portable Ice Nucleation Experiment during the Pallas Cloud Experiment 2022, https://doi.org/10.5281/zenodo.13889647, 2024.

Ceppi, P., Brient, F., Zelinka, M., and Hartmann, D.: Cloud feedback mechanisms and their representation in global climate models, Wiley Interdiscip Rev Clim, 8, https://doi.org/10.1002/wcc.465, 2017.

Christner, B. C., Cai, R., Morris, C. E., McCarter, K. S., Foreman, C. M., Skidmore, M. L., Montross, S. N., and Sands, D. C.: Geographic, seasonal, and precipitation chemistry influence on the abundance and activity of biological ice nucleators in rain and snow, Proc Natl Acad Sci, 105, 18 854–18 859, https://doi.org/10.1073/pnas.0809816105, 2008.

Clancy, J. H., Markey, E., Martínez-Bracero, M., Maya-Manzano, J. M., McGillicuddy, E. J., Sewell, G., Sarda-Estève, R., Baisnée, D., Vélez-Pereira, A. M., Davis, G., and O'Connor, D. J.: Comparative Analysis of Real-Time Fluorescence-Based Spectroscopic Instruments: Bioaerosol Detection in the Urban Environment of Dublin City, Ireland, Atmosphere, 16, https://doi.org/10.3390/atmos16030275, 2025.

Cohen, J., Screen, J. A., Furtado, J. C., Barlow, M., Whittleston, D., Coumou, D., Francis, J., Dethloff, K., Entekhabi, D., Overland, J., and Jones, J.: Recent Arctic amplification and extreme mid-latitude weather, Nature Geoscience, 7, 627–637, https://doi.org/10.1038/ngeo2234, 2014.

Cornwell, G. C., McCluskey, C. S., Hill, T. C. J., Levin, E. T., Rothfuss, N. E., Tai, S.-L., Petters, M. D., DeMott, P. J., Kreidenweis, S., Prather, K. A., and Burrows, S. M.: Bioaerosols are the dominant source of warm-temperature immersion-mode INPs and drive uncertainties in INP predictability, Sci Adb, 9, eadg3715, https://doi.org/10.1126/sciadv.adg3715, 2023.

Daily, M. I., Tarn, M., Whale, T., and Murray, B.: An evaluation of the heat test for the ice-nucleating ability of minerals and biological material, Atmos Meas Tech, https://doi.org/10.5194/amt-15-2635-2022, 2022.

Dankers, R. and Christensen, O. B.: Climate Change Impact on Snow Coverage, Evaporation and River Discharge in the Sub-Arctic Tana Basin, Northern Fennoscandia, Climatic Change, 69, 367–392, https://doi.org/10.1007/s10584-005-2533-y, 2005.

De Groot, R. C.: Diurnal cycles of airborne spores produced by forest fungi., 58, 1223–1229, 1968.

DeMott, P. J. and Prenni, A. J.: New Directions: Need for defining the numbers and sources of biological aerosols acting as ice nuclei, Atmos Environ, 44, 1944–1945, https://doi.org/10.1016/j.atmosenv.2010.02.032, 2010.

DeMott, P. J., Sassen, K., Poellot, M. R., Baumgardner, D., Rogers, D. C., Brooks, S. D., Prenni, A. J., and Kreidenweis, S. M.: African dust aerosols as atmospheric ice nuclei, Geophys Res Lett, 30, https://doi.org/10.1029/2003GL017410, 2003.

Diehl, K., Quick, C., Matthias-Maser, S., Mitra, S., and Jaenicke, R.: The ice nucleating ability of pollen: Part I: Laboratory studies in deposition and condensation freezing modes, Atmospheric Research, 58, 75–87, https://doi.org/10.1016/S0169-8095(01)00091-6, 2001.

Doulgeris, K. M., Lihavainen, H., Hyvärinen, A.-P., Kerminen, V.-M., and Brus, D.: An extensive data set for in situ microphysical characterization of low-level clouds in a Finnish sub-Arctic site, Earth Syst Sci Data, 14, 637–649, https://doi.org/10.5194/essd-14-637-2022, 2022.

Drinovec, L., Močnik, G., Zotter, P., Prévôt, A. S. H., Ruckstuhl, C., Coz, E., Rupakheti, M., Sciare, J., Müller, T., Wiedensohler, A., and Hansen, A. D. A.: The "dual-spot" Aethalometer: an improved measurement of aerosol black carbon with real-time loading compensation, Atmos Meas Tech, 8, 1965–1979, https://doi.org/10.5194/amt-8-1965-2015, 2015.

Edgar, R. C.: Search and clustering orders of magnitude faster than BLAST, Bioinformatics, 26, 2460–2461, https://doi.org/10.1093/bioinformatics/btq461, 2010.

Elbert, W., Taylor, P. E., Andreae, M. O., and Pöschl, U.: Contribution of fungi to primary biogenic aerosols in the atmosphere: wet and dry discharged spores, carbohydrates, and inorganic ions, Atmos Chem Phys, 7, 4569–4588, https://doi.org/10.5194/acp-7-4569-2007, 2007.

Failor, K. C., Schmale, D., Vinatzer, B., Monteil, C., Monteil, C., and Monteil, C.: Ice nucleation active bacteria in precipitation are genetically diverse and nucleate ice by employing different mechanisms, The ISME Journal, 11, 2740–2753, https://doi.org/10.1038/ismej.2017.124, 2017.

Fernández-Rodríguez, S., Tormo-Molina, R., Lemonis, N., Clot, B., O'Connor, D., and Sodeau, J. R.: Comparison of fungal spores concentrations measured with wideband integrated bioaerosol sensor and Hirst methodology, Atmos Environ, 175, 1–14, https://doi.org/10.1016/j.atmosenv.2017.11.038, 2018.

Fröhlich-Nowoisky, J., Burrows, S. M., Xie, Z., Engling, G., Solomon, P. A., Fraser, M. P., Mayol-Bracero, O. L., Artaxo, P., Begerow, D., Conrad, R., Andreae, M. O., Després, V. R., and Pöschl, U.: Biogeography in the air: fungal diversity over land and oceans, Biogeosciences, 9, 1125–1136, https://doi.org/10.5194/bg-9-1125-2012, 2012.

Fröhlich-Nowoisky, J., Hill, T. C. J., Pummer, B. G., Yordanova, P., Franc, G. D., and Pöschl, U.: Ice nucleation activity in the widespread soil fungus Mortierella alpina, Biogeosciences, 12, 1057–1071, https://doi.org/10.5194/bg-12-1057-2015, 2015.

Fröhlich-Nowoisky, J., Pickersgill, D. A., Després, V. R., and Pöschl, U.: High diversity of fungi in air particulate matter, Proc Natl Acad Sci, 106, 12 814–12 819, https://doi.org/10.1073/pnas.0811003106, 2009.

Fröhlich-Nowoisky, J., Kampf, C. J., Weber, B., Huffman, J. A., Pöhlker, C., Andreae, M. O., Lang-Yona, N., Burrows, S. M., Gunthe, S. S., Elbert, W., Su, H., Hoor, P., Thines, E., Hoffmann, T., Després, V. R., and Pöschl, U.: Bioaerosols in the Earth system: Climate, health, and ecosystem interactions, Atmos Res, 182, 346–376, https://doi.org/10.1016/j.atmosres.2016.07.018, 2016.

Fu, P. Q., Kawamura, K., Chen, J., Charrière, B., and Sempéré, R.: Organic molecular composition of marine aerosols over the Arctic Ocean in summer: contributions of primary emission and secondary aerosol formation, Biogeosciences, 10, 653–667, https://doi.org/10.5194/bg-10-653-2013, 2013.

Gabey, A., Gallagher, M., Whitehead, J., Dorsey, J., Kaye, P. H., and Stanley, W.: Measurements and comparison of primary biological aerosol above and below a tropical forest canopy using a dual channel fluorescence spectrometer, Atmos Chem Phys, 10, 4453–4466, https://doi.org/10.5194/acp-10-4453-2010, 2010.

Gao, K., Vogel, F., Foskinis, R., Vratolis, S., Gini, M. I., Granakis, K., Billault-Roux, A.-C., Georgakaki, P., Zografou, O., Fetfatzis, P., Berne, A., Papayannis, A., Eleftheridadis, K., Möhler, O., and Nenes, A.: Biological and dust aerosols as sources of ice-nucleating particles in the eastern Mediterranean: source apportionment, atmospheric processing and parameterization, Atmos Chem Phys, 24, 9939–9974, https://doi.org/10.5194/acp-24-9939-2024, 2024.

Garcia, E., Hill, T. C. J., Prenni, A. J., DeMott, P. J., Franc, G. D., and Kreidenweis, S. M.: Biogenic ice nuclei in boundary layer air over two U.S. High Plains agricultural regions, J Geophys Res, 117, https://doi.org/10.1029/2012JD018343, 2012.

Gilbert, G. S. and Reynolds, D. R.: Nocturnal Fungi: Airborne Spores in the Canopy and Understory of a Tropical Rain Forest, Biotropica, 37, 462–464, https://doi.org/10.1111/j.1744-7429.2005.00061.x, 2005.

Gjelsvik, A. B., David, R. O., Carlsen, T., Hellmuth, F., Hofer, S., McGraw, Z., Sodemann, H., and Storelvmo, T.: Using a region-specific ice-nucleating particle parameterization improves the representation of Arctic clouds in a global climate model, Atmos Chem Phys, 25, 1617–1637, https://doi.org/10.5194/acp-25-1617-2025, 2025.

Gorfer, M., Mayer, M., Berger, H., Rewald, B., Tallian, C., Matthews, B., Sandén, H., Katzensteiner, K., and Godbold, D. L.: High Fungal Diversity but Low Seasonal Dynamics and Ectomycorrhizal Abundance in a Mountain Beech Forest, Microb Ecol, 82, 243–256, https://doi.org/10.1007/s00248-021-01736-5, 2021.

Gosselin, M. I., Rathnayake, C. M., Crawford, I., Pöhlker, C., Fröhlich-Nowoisky, J., Schmer, B., Després, V. R., Engling, G., Gallagher, M., Stone, E., Pöschl, U., and Huffman, J. A.: Fluorescent bioaerosol particle, molecular tracer, and fungal spore concentrations during dry and rainy periods in a semi-arid forest, Atmos Chem Phys, 16, 15 165–15 184, https://doi.org/10.5194/acp-16-15165-2016, 2016.

Gratzl, J.: Data of Fluorescent Aerosol Particles during the Pallas Cloud Experiment 2022, https://doi.org/10.5281/zenodo.13885888, 2024.

Gratzl, J. and Grothe, H.: Highly fluorescent aerosol particle and fungal DNA data collected in Pallas from April to September 2023, https://doi.org/10.48436/0xmsb-eps20, 2025.

Gratzl, J., Brus, D., Doulgeris, K., Böhmländer, A., Möhler, O., and Grothe, H.: Fluorescent aerosol particles in the Finnish sub-Arctic during the Pallas Cloud Experiment 2022 campaign, Earth Syst Sci Data Discuss, 2025, 1–20, https://doi.org/10.5194/essd-2024-543, 2025.

Haga, D. I., Iannone, R., Wheeler, M. J., Mason, R., Polishchuk, E. A., Fetch Jr., T., van der Kamp, B. J., McKendry, I. G., and Bertram, A. K.: Ice nucleation properties of rust and bunt fungal spores and their transport to high altitudes, where they can cause heterogeneous freezing, J Geophys Res, 118, 7260–7272, https://doi.org/10.1002/jgrd.50556, 2013.

Haga, D. I., Burrows, S. M., Iannone, R., Wheeler, M. J., Mason, R. H., Chen, J., Polishchuk, E. A., Pöschl, U., and Bertram, A. K.: Ice nucleation by fungal spores from the classes Agaricomycetes, Ustilaginomycetes, and Eurotiomycetes, and the effect on the atmospheric transport of these spores, Atmos Chem Phys, 14, 8611–8630, https://doi.org/10.5194/acp-14-8611-2014, 2014.

Halbritter, H., Heigl, H., and W., A.: Pinus Sylvestris, PalDat - A palynological database, https://doi.org/https://www.paldat.org/pub/Pinus_sylvestris/306147, accessed 2025-02-14, 2021.

Hartmann, M., Gong, X., Kecorius, S., van Pinxteren, M., Vogl, T., Welti, A., Wex, H., Zeppenfeld, S., Herrmann, H., Wiedensohler, A., and Stratmann, F.: Terrestrial or marine – indications towards the origin of ice-nucleating particles during melt season in the European Arctic

770   up to 83.7° N, Atmos Chem Phys, 21, 11 613–11 636, https://doi.org/10.5194/acp-21-11613-2021, 2021.

Hatakka, J., Aalto, T., Aaltonen, V., Aurela, M., Hakola, H., Komppula, M., Laurila, T., Lihavainen, H., Paatero, J., Salminen, K., et al.: Overview of the atmospheric research activities and results at Pallas GAW station, Boreal Environ Res, 8, 365, 2003.

Hawksworth, D. L. and Lücking, R.: Fungal Diversity Revisited: 2.2 to 3.8 Million Species, Microbiol Spectr, 5, https://doi.org/10.1128/microbiolspec.funk-0052-2016, 2017.

775   Healy, D., Huffman, J., O'Connor, D. J., Pöhlker, C., Pöschl, U., and Sodeau, J.: Ambient measurements of biological aerosol particles near Killarney, Ireland: a comparison between real-time fluorescence and microscopy techniques, Atmos Chem Phys, 14, 8055–8069, https://doi.org/10.5194/acp-14-8055-2014, 2014.

Helin, A., Sietiö, O.-M., Heinonsalo, J., Bäck, J., Riekkola, M.-L., and Parshintsev, J.: Characterization of free amino acids, bacteria and fungi in size-segregated atmospheric aerosols in boreal forest: seasonal patterns, abundances and size distributions, Atmos Chem Phys,

780   17, 13 089–13 101, https://doi.org/10.5194/acp-17-13089-2017, 2017.

Herbert, R. J., Sanchez-Marroquin, A., Grosvenor, D. P., Pringle, K. J., Arnold, S. R., Murray, B. J., and Carslaw, K. S.: Gaps in our understanding of ice-nucleating particle sources exposed by global simulation of the UK Earth System Model, Atmos Chem Phys, 25, 291–325, https://doi.org/10.5194/acp-25-291-2025, 2025.

Hernandez, M., Perring, A. E., McCabe, K., Kok, G., Granger, G., and Baumgardner, D.: Chamber catalogues of optical and fluorescent

785   signatures distinguish bioaerosol classes, Atmos Meas Tech, 9, 3283–3292, https://doi.org/10.5194/amt-9-3283-2016, 2016.

Hill, T. C. J., DeMott, P. J., Tobo, Y., Fröhlich-Nowoisky, J., Moffett, B. F., Franc, G. D., and Kreidenweis, S. M.: Sources of organic ice nucleating particles in soils, Atmospheric Chemistry and Physics, 16, 7195–7211, https://doi.org/10.5194/acp-16-7195-2016, 2016.

Hirst, J. M.: AN AUTOMATIC VOLUMETRIC SPORE TRAP, Ann Appl Biol, 39, 257–265, https://doi.org/10.1111/j.1744-7348.1952.tb00904.x, 1952.

790   Hofstetter, V., Buyck, B., Eyssartier, G., Schnee, S., and Gindro, K.: The unbearable lightness of sequenced-based identification, Fungal Diversity, 96, 243–284, https://doi.org/10.1007/s13225-019-00428-3, 2019.

Huang, S., Hu, W., Chen, J., Wu, Z., Zhang, D., and Fu, P.: Overview of biological ice nucleating particles in the atmosphere, Environ Int, 146, 106 197, https://doi.org/10.1016/j.envint.2020.106197, 2021.

Huffman, J. A., Prenni, A., DeMott, P., Pöhlker, C., Mason, R., Robinson, N., Fröhlich-Nowoisky, J., Tobo, Y., Després, V., Garcia, E.,

795   et al.: High concentrations of biological aerosol particles and ice nuclei during and after rain, Atmos Chem Phys, 13, 6151–6164, https://doi.org/10.5194/acp-13-6151-2013, 2013.

Hughes, D. D., Mampage, C. B., Jones, L. M., Liu, Z., and Stone, E. A.: Characterization of atmospheric pollen fragments during springtime thunderstorms, Environ Sci Technol Lett, 7, 409–414, https://doi.org/10.1021/acs.estlett.0c00213, 2020.

Iannone, R., Chernoff, D. I., Pringle, A., Martin, S. T., and Bertram, A. K.: The ice nucleation ability of one of the most abundant types of

800   fungal spores found in the atmosphere, Atmos Chem Phys, 11, 1191–1201, https://doi.org/10.5194/acp-11-1191-2011, 2011.

Irish, V. E., Hanna, S. J., Willis, M. D., China, S., Thomas, J. L., Wentzell, J. J. B., Cirisan, A., Si, M., Leaitch, W. R., Murphy, J. G., Abbatt, J. P. D., Laskin, A., Girard, E., and Bertram, A. K.: Ice nucleating particles in the marine boundary layer in the Canadian Arctic during summer 2014, Atmos Chem Phys, 19, 1027–1039, https://doi.org/10.5194/acp-19-1027-2019, 2019.

Jayaweera, K. and Flanagan, P.: Investigations on biogenic ice nuclei in the Arctic atmosphere, Geophys Res Lett, 9, 94–97, https://doi.org/10.1029/GL009i001p00094, 1982.

Joly, M., Attard, E., Sancelme, M., Deguillaume, L., Guilbaud, C., Morris, C. E., Amato, P., and Delort, A.-M.: Ice nucleation activity of bacteria isolated from cloud water, Atmos Environ, 70, 392–400, https://doi.org/10.1016/j.atmosenv.2013.01.027, 2013.

Kabir, E., Azzouz, A., Raza, N., Bhardwaj, S., Kim, K., Tabatabaei, M., and Kukkar, D.: Recent advances in monitoring, sampling, and sensing techniques for bioaerosols in the atmosphere., ACS sensors, https://doi.org/10.1021/acssensors.9b02585, 2020.

Kanji, Z. A., Ladino, L. A., Wex, H., Boose, Y., Burkert-Kohn, M., Cziczo, D. J., and Krämer, M.: Overview of Ice Nucleating Particles, Meteorol Monogr, 58, 1.1 – 1.33, https://doi.org/10.1175/AMSMONOGRAPHS-D-16-0006.1, 2017.

Kawana, K., Taketani, F., Matsumoto, K., Tobo, Y., Iwamoto, Y., Miyakawa, T., Ito, A., and Kanaya, Y.: Roles of marine biota in the formation of atmospheric bioaerosols, cloud condensation nuclei, and ice-nucleating particles over the North Pacific Ocean, Bering Sea, and Arctic Ocean, Atmos Chem Phys, 24, 1777–1799, https://doi.org/10.5194/acp-24-1777-2024, 2024.

Köppen, W. P.: Grundriss der klimakunde, W. de Gruyter, 1931.

Krupodorova, T., Barshteyn, V., and Sekan, A.: Review of the basic cultivation conditions influence on the growth of basidiomycetes, Current Research in Environmental Applied Mycology, https://doi.org/10.5943/cream/11/1/34, 2021.

Kunert, A. T., Pöhlker, M. L., Tang, K., Krevert, C. S., Wieder, C., Speth, K. R., Hanson, L. E., Morris, C. E., Schmale III, D. G., Pöschl, U., and Fröhlich-Nowoisky, J.: Macromolecular fungal ice nuclei in Fusarium: effects of physical and chemical processing, Biogeosciences, 16, 4647–4659, https://doi.org/10.5194/bg-16-4647-2019, 2019.

Lacher, L., Clemen, H.-C., Shen, X., Mertes, S., Gysel-Beer, M., Moallemi, A., Steinbacher, M., Henne, S., Saathoff, H., Möhler, O., et al.: Sources and nature of ice-nucleating particles in the free troposphere at Jungfraujoch in winter 2017, Atmos Chem Phys, 21, 16 925–16 953, https://doi.org/10.5194/acp-21-16925-2021, 2021.

Lohila, A., Penttilä, T., Jortikka, S., Aalto, T., Anttila, P., Asmi, E., Aurela, M., Hatakka, J., Hellén, H., Henttonen, H., Hänninen, P., Kilkki, J., Kyllönen, K., Laurila, T., Lepistö, A., Lihavainen, H., Makkonen, U., Paatero, J., Rask, M., and Viisanen, Y.: Preface to the special issue on integrated research of atmosphere, ecosystems and environment at Pallas, Boreal Environ Res, 20, 431–454, 2015.

Maki, L., Galyan, E., Chang-Chien, M., and Caldwell, D.: Ice nucleation induced by pseudomonas syringae, Appl Microbiol, 28, 456—459, https://doi.org/10.1128/am.28.3.456-459.1974, 1974.

Maki, L. R. and Willoughby, K. J.: Bacteria as Biogenic Sources of Freezing Nuclei, J Appl Meteorol Climatol, 17, 1049 – 1053, https://doi.org/10.1175/1520-0450(1978)017<1049:BABSOF>2.0.CO;2, 1978.

Maki, T., Hosaka, K., Lee, K. C., Kawabata, Y., Kajino, M., Uto, M., Kita, K., and Igarashi, Y.: Vertical distribution of airborne microorganisms over forest environments: A potential source of ice-nucleating bioaerosols, Atmos Environ, 302, 119 726, https://doi.org/10.1016/j.atmosenv.2023.119726, 2023.

Mäkinen, Y.: Random sampling in the study of microscopic slides, Rep Aerobiol Lab Univ Turku, 5, 27–43, 1981.

Mampage, C. B., Hughes, D. D., Jones, L. M., Metwali, N., Thorne, P. S., and Stone, E. A.: Characterization of sub-pollen particles in size-resolved atmospheric aerosol using chemical tracers, Atmos Environ: X, 15, 100 177, https://doi.org/10.1016/j.aeaoa.2022.100177, 2022.

Markey, E., Hourihane Clancy, J., Martínez-Bracero, M., Neeson, F., Sarda-Estève, R., Baisnée, D., McGillicuddy, E. J., Sewell, G., and O'Connor, D. J.: A Modified Spectroscopic Approach for the Real-Time Detection of Pollen and Fungal Spores at a Semi-Urban Site Using the WIBS-4+, Part I, Ah S Sens, 22, https://doi.org/10.3390/s22228747, 2022.

Markey, E., Hourihane Clancy, J., Martínez-Bracero, M., Sarda-Estève, R., Baisnée, D., McGillicuddy, E. J., Sewell, G., Skjøth, C. A., and O'Connor, D. J.: Spectroscopic detection of bioaerosols with the wibs-4+: Anthropogenic and meteorological impacts, Sci Total Environ, 943, 173 649, https://doi.org/https://doi.org/10.1016/j.scitotenv.2024.173649, 2024.

Mason, R., Si, M., Li, J., Chou, C., Dickie, R., Toom-Sauntry, D., Pöhlker, C., Yakobi-Hancock, J., Ladino, L., Jones, K., et al.: Ice nucleating
845   particles at a coastal marine boundary layer site: correlations with aerosol type and meteorological conditions, Atmos Chem Phys, 15, 12 547–12 566, https://doi.org/10.5194/acp-15-12547-2015, 2015.

Mason, R. H., Si, M., Chou, C., Irish, V. E., Dickie, R., Elizondo, P., Wong, R., Brintnell, M., Elsasser, M., Lassar, W. M., Pierce, K. M., Leaitch, W. R., MacDonald, A. M., Platt, A., Toom-Sauntry, D., Sarda-Estève, R., Schiller, C. L., Suski, K. J., Hill, T. C. J., Abbatt, J. P. D., Huffman, J. A., DeMott, P. J., and Bertram, A. K.: Size-resolved measurements of ice-nucleating particles at six locations in North
850   America and one in Europe, Atmos Chem Phys, 16, 1637–1651, https://doi.org/10.5194/acp-16-1637-2016, 2016.

Masson-Delmotte, V., Zhai, P., Pirani, A., Connors, S. L., Péan, C., Berger, S., Caud, N., Chen, Y., Goldfarb, L., Gomis, M., et al.: Climate change 2021: the physical science basis, Contribution of working group I to the sixth assessment report of the intergovernmental panel on climate change, 2, 2391, 2021.

Matthews, B. H., Alsante, A. N., and Brooks, S. D.: Pollen Emissions of Subpollen Particles and Ice Nucleating Particles, ACS Earth Space
855   Chem, 7, 1207–1218, https://doi.org/10.1021/acsearthspacechem.3c00014, 2023.

McMurdie, P. J. and Holmes, S.: phyloseq: An R Package for Reproducible Interactive Analysis and Graphics of Microbiome Census Data, PLoS ONE, 8, e61 217, https://doi.org/10.1371/journal.pone.0061217, 2013.

Mikryukov, V. and Mahé, F.: vmikk/metagMisc: 0.5.0, https://doi.org/10.5281/zenodo.15060881, 2025.

Möhler, O., Adams, M., Lacher, L., Vogel, F., Nadolny, J., Ullrich, R., Boffo, C., Pfeuffer, T., Hobl, A., Weiß, M., et al.: The Portable
860   Ice Nucleation Experiment (PINE): a new online instrument for laboratory studies and automated long-term field observations of ice-nucleating particles, Atmos Meas Tech, 14, 1143–1166, https://doi.org/10.5194/amt-2020-307, 2021.

Morris, C. E., Georgakopoulos, D. G., and Sands, D. C.: Ice nucleation active bacteria and their potential role in precipitation, in: Journal de Physique IV (Proceedings), vol. 121, pp. 87–103, EDP sciences, https://doi.org/10.1051/jp4:2004121004, 2004.

Morris, C. E., Sands, D. C., Glaux, C., Samsatly, J., Asaad, S., Moukahel, A. R., Gonçalves, F. L. T., and Bigg, E. K.: Urediospores
865   of rust fungi are ice nucleation active at > -10 °C and harbor ice nucleation active bacteria, Atmos Chem Phys, 13, 4223–4233, https://doi.org/10.5194/acp-13-4223-2013, 2013.

Murray, B. J., O'Sullivan, D., Atkinson, J. D., and Webb, M. E.: Ice nucleation by particles immersed in supercooled cloud droplets, Chem Soc Rev, 41, 6519–6554, https://doi.org/10.1039/C2CS35200A, 2012.

Murray, B. J., Carslaw, K. S., and Field, P. R.: Opinion: Cloud-phase climate feedback and the importance of ice-nucleating particles, Atmos
870   Chem Phys, 21, 665–679, https://doi.org/10.5194/acp-21-665-2021, 2021.

Niu, M., Hu, W., Huang, S., Chen, J., Zhong, S., Huang, Z., Duan, P., Pei, X., Duan, J., Bi, K., Chen, S., Jin, R., Sheng, M., Yang, N., Wu, L., Deng, J., Zhu, J., Shen, F., Wu, Z., Zhang, D., and Fu, P.: Deciphering the Significant Role of Biological Ice Nucleators in Precipitation at the Organic Molecular Level, J Geophys Res: Atmos, 129, e2024JD041 278, https://doi.org/10.1029/2024JD041278, e2024JD041278 2024JD041278, 2024.

875 Oksanen, J., Blanchet, F. G., Friendly, M., Kindt, R., Legendre, P., McGlinn, D., Minchin, P. R., O'Hara, R. B., Simpson, G. L., Solymos, P., Stevens, M. H. H., Szoecs, E., and Wagner, H.: Package "vegan", https://cran.r-project.org/web/packages/vegan/vegan.pdf, r Package version 2.0-8, 2018.

O'Connor, D. J., Healy, D. A., and Sodeau, J. R.: A 1-month online monitoring campaign of ambient fungal spore concentrations in the harbour region of Cork, Ireland, Aerobiologia, 31, 295–314, https://doi.org/10.1007/s10453-015-9365-7, 2015.

880 O'Sullivan, D., Adams, M. P., Tarn, M. D., Harrison, A. D., Vergara-Temprado, J., Porter, G. C. E., Holden, M. A., Sanchez-Marroquin, A., Carotenuto, F., Whale, T. F., McQuaid, J. B., Walshaw, R., Hedges, D. H. P., Burke, I. T., Cui, Z., and Murray, B. J.: Contributions of biogenic material to the atmospheric ice-nucleating particle population in North Western Europe, Sci Rep, 8, 13 821, https://doi.org/10.1038/s41598-018-31981-7, 2018.

Pan, Y.-L., Kalume, A., Wang, C., and Santarpia, J.: Atmospheric aging processes of bioaerosols under laboratory-controlled conditions: A
885 review, J Aerosol Sci, 155, 105 767, https://doi.org/10.1016/j.jaerosci.2021.105767, 2021.

Paramonov, M., Drossaart van Dusseldorp, S., Gute, E., Abbatt, J. P. D., Heikkilä, P., Keskinen, J., Chen, X., Luoma, K., Heikkinen, L., Hao, L., Petäjä, T., and Kanji, Z. A.: Condensation/immersion mode ice-nucleating particles in a boreal environment, Atmos Chem Phys, 20, 6687–6706, https://doi.org/10.5194/acp-20-6687-2020, 2020.

Pashley, C. H., Fairs, A., Free, R. C., and Wardlaw, A. J.: DNA analysis of outdoor air reveals a high degree of fungal diversity, temporal
890 variability, and genera not seen by spore morphology, Fungal Biology, 116, 214–224, https://doi.org/10.1016/j.funbio.2011.11.004, 2012.

Pereira Freitas, G., Adachi, K., Conen, F., Heslin-Rees, D., Krejci, R., Tobo, Y., Yttri, K. E., and Zieger, P.: Regionally sourced bioaerosols drive high-temperature ice nucleating particles in the Arctic, Nat Commun, 14, 5997, https://doi.org/10.1038/s41467-023-41696-7, 2023.

Perring, A., Schwarz, J., Baumgardner, D., Hernandez, M., Spracklen, D., Heald, C., Gao, R., Kok, G., McMeeking, G., McQuaid, J., et al.: Airborne observations of regional variation in fluorescent aerosol across the United States, J Geophys Res-Atmos, 120, 1153–1170,
895 https://doi.org/10.1002/2014JD022495, 2015.

Petersson Sjögren, M., Alsved, M., Šantl Temkiv, T., Bjerring Kristensen, T., and Löndahl, J.: Measurement report: Atmospheric fluorescent bioaerosol concentrations measured during 18 months in a coniferous forest in the south of Sweden, Atmos Chem Phys, 23, 4977–4992, https://doi.org/10.5194/acp-23-4977-2023, 2023.

Pouleur, S., Richard, C., Martin, J.-G., and Antoun, H.: Ice Nucleation Activity in *Fusarium acuminatum* and *Fusarium avenaceum*, Appl
900 Environ Microbiol, 58, 2960–2964, https://doi.org/10.1128/aem.58.9.2960-2964.1992, 1992.

Prenni, A., Tobo, Y., Garcia, E., DeMott, P., Huffman, J., McCluskey, C., Kreidenweis, S., Prenni, J., Pöhlker, C., and Pöschl, U.: The impact of rain on ice nuclei populations at a forested site in Colorado, Geophys Res Lett, 40, 227–231, https://doi.org/10.1029/2012GL053953, 2013.

Pringle, A., Patek, S. N., Fischer, M., Stolze, J., and Money, N. P.: The Captured Launch of a Ballistospore, Mycologia, 97, 866–871,
905 http://www.jstor.org/stable/3762235, 2005.

Pruppacher, H. R., Klett, J. D., and Wang, P. K.: Microphysics of clouds and precipitation, 1998.

Pummer, B. G., Bauer, H., Bernardi, J., Bleicher, S., and Grothe, H.: Suspendable macromolecules are responsible for ice nucleation activity of birch and conifer pollen, Atmos Chem Phys, 12, 2541–2550, https://doi.org/10.5194/acp-12-2541-2012, 2012.

Pummer, B. G., Atanasova, L., Bauer, H., Bernardi, J., Druzhinina, I. S., Fröhlich-Nowoisky, J., and Grothe, H.: Spores of many
910 common airborne fungi reveal no ice nucleation activity in oil immersion freezing experiments, Biogeosciences, 10, 8083–8091, https://doi.org/10.5194/bg-10-8083-2013, 2013.

Pummer, B. G., Budke, C., Augustin-Bauditz, S., Niedermeier, D., Felgitsch, L., Kampf, C. J., Huber, R. G., Liedl, K. R., Loerting, T., Moschen, T., Schauperl, M., Tollinger, M., Morris, C. E., Wex, H., Grothe, H., Pöschl, U., Koop, T., and Fröhlich-Nowoisky, J.: Ice nucleation by water-soluble macromolecules, Atmos Chem Phys, 15, 4077–4091, https://doi.org/10.5194/acp-15-4077-2015, 2015.

915 Qu, Z.-L., Santalahti, M., Köster, K., Berninger, F., Pumpanen, J., Heinonsalo, J., and Sun, H.: Soil Fungal Community Structure in Boreal
Pine Forests: From Southern to Subarctic Areas of Finland, Front Microbiol, 12, https://doi.org/10.3389/fmicb.2021.653896, 2021.

Raimondi, V., Agati, G., Cecchi, G., Gomoiu, I., Lognoli, D., and Palombi, L.: In vivo real-time recording of UV-induced changes in the
autofluorescence of a melanin-containing fungus using a micro-spectrofluorimeter and a low-cost webcam, Opt Express, 17, 22 735–
22 746, https://doi.org/10.1364/OE.17.022735, 2009.

920 Rantanen, M., Karpechko, A. Y., Lipponen, A., Nordling, K., Hyvärinen, O., Ruosteenoja, K., Vihma, T., and Laaksonen, A.: The Arctic has
warmed nearly four times faster than the globe since 1979, Commun Earth Environ, 3, 168, https://doi.org/10.1038/s43247-022-00498-3,
2022.

Rognes, T., Flouri, T., Nichols, B., Quince, C., and Mahé, F.: VSEARCH: a versatile open source tool for metagenomics, PeerJ, 4, e2584,
2016.

925 Rolph, G., Stein, A., and Stunder, B.: Real-time Environmental Applications and Display sYstem: READY, Environmental Modelling Soft-
ware, 95, 210–228, https://doi.org/10.1016/j.envsoft.2017.06.025, 2017.

Rungjindamai, N. and Jones, E. B. G.: Why Are There So Few Basidiomycota and Basal Fungi as Endophytes? A Review, Journal of Fungi,
10, https://doi.org/10.3390/jof10010067, 2024.

Sarangi, B., Baumgardner, D., Bolaños Rosero, B., and Mayol-Bracero, O. L.: Measurement report: An exploratory study of fluo-
930 rescence and cloud condensation nuclei activity of urban aerosols in San Juan, Puerto Rico, Atmos Chem Phys, 22, 9647–9661,
https://doi.org/10.5194/acp-22-9647-2022, 2022.

Savage, N. J., Krentz, C. E., Könemann, T., Han, T. T., Mainelis, G., Pöhlker, C., and Huffman, J. A.: Systematic characterization and
fluorescence threshold strategies for the wideband integrated bioaerosol sensor (WIBS) using size-resolved biological and interfering
particles, Atmos Meas Tech, 10, 4279–4302, https://doi.org/10.5194/amt-10-4279-2017, 2017.

935 Schleh, C., Erpenbeck, V. J., Winkler, C., Lauenstein, H. D., Nassimi, M., Braun, A., Krug, N., and Hohlfeld, J. M.: Allergen par-
ticle binding by human primary bronchial epithelial cells is modulated by surfactant protein D, Respiratory Research, 11, 83,
https://doi.org/10.1186/1465-9921-11-83, 2010.

Schneider, J., Höhler, K., Heikkilä, P., Keskinen, J., Bertozzi, B., Bogert, P., Schorr, T., Umo, N. S., Vogel, F., Brasseur, Z., Wu, Y., Hakala,
S., Duplissy, J., Moisseev, D., Kulmala, M., Adams, M. P., Murray, B. J., Korhonen, K., Hao, L., Thomson, E. S., Castarède, D., Leisner,
940 T., Petäjä, T., and Möhler, O.: The seasonal cycle of ice-nucleating particles linked to the abundance of biogenic aerosol in boreal forests,
Atmos Chem Phys, 21, 3899–3918, https://doi.org/10.5194/acp-21-3899-2021, 2021.

Schnell, R. C. and Vali, G.: Biogenic Ice Nuclei: Part I. Terrestrial and Marine Sources, J Atmos sci, 33, 1554 – 1564, https://journals.
ametsoc.org/view/journals/atsc/33/8/1520-0469_1976_033_1554_binpit_2_0_co_2.xml, 1976.

Schumacher, C., Pöhlker, C., Aalto, P., Hiltunen, V., Petäjä, T., Kulmala, M., Pöschl, U., and Huffman, J.: Seasonal cycles of fluo-
945 rescent biological aerosol particles in boreal and semi-arid forests of Finland and Colorado, Atmos Chem Phys, 13, 11 987–12 001,
https://doi.org/10.5194/acp-13-11987-2013, 2013.

Screen, J. A. and Simmonds, I.: The central role of diminishing sea ice in recent Arctic temperature amplification, Nature, 464, 1334–1337,
https://doi.org/10.1038/nature09051, 2010.

Serreze, M. C. and Barry, R. G.: Processes and impacts of Arctic amplification: A research synthesis, Global Planet Change, 77, 85–96,
950 https://doi.org/10.1016/j.gloplacha.2011.03.004, 2011.

Stein, A. F., Draxler, R. R., Rolph, G. D., Stunder, B. J. B., Cohen, M. D., and Ngan, F.: NOAA's HYSPLIT Atmospheric Transport and
Dispersion Modeling System, Bull Am Meteorol Soc, 96, 2059 – 2077, https://doi.org/10.1175/BAMS-D-14-00110.1, 2015.

Stephanie and Waturangi, D. E.: Distribution of Ice Nucleation-Active (INA) Bacteria from Rain-water and Air, HAYATI J Biosci, 18, 108–112, https://doi.org/10.4308/hjb.18.3.108, 2011.

955 Sterkenburg, E., Bahr, A., Durling, M. B., Clemmensen, K. E., and Lindahl, B. D.: Changes in fungal communities along a boreal forest soil fertility gradient., The New phytologist, 207 4, 1145–58, https://doi.org/10.1111/nph.13426, 2015.

Stone, E. A., Mampage, C. B., Hughes, D. D., and Jones, L. M.: Airborne sub-pollen particles from rupturing giant ragweed pollen, Aerobiologia, pp. 1–8, https://doi.org/10.1007/s10453-021-09702-x, 2021.

Suphioglu, C., Singh, M. B., Taylor, P., Bellomo, R., Holmes, P., Puy, R., and Knox, R. B.: Mechanism of grass-pollen-induced asthma., 960 Lancet (London, England), 339, 569–72, https://doi.org/10.1016/0140-6736(92)90864-y, 1992.

Taketani, F., Tobo, Y., Miyakawa, T., Takigawa, M., Zhu, C., and Kanaya, Y.: Impact of Siberian Wildfires on Ice-Nucleating Particle Concentrations over the Northwestern Pacific, Environ Sci Technol, https://doi.org/10.1021/acs.est.4c04889, 2025.

Tan, I., Barahona, D., and Coopman, Q.: Potential Link Between Ice Nucleation and Climate Model Spread in Arctic Amplification, Geophy Res Lett, 49, https://doi.org/10.1029/2021GL097373, 2022.

965 Tang, K., Sánchez-Parra, B., Yordanova, P., Wehking, J., Backes, A. T., Pickersgill, D. A., Maier, S., Sciare, J., Pöschl, U., Weber, B., and Fröhlich-Nowoisky, J.: Bioaerosols and atmospheric ice nuclei in a Mediterranean dryland: community changes related to rainfall, Biogeosciences, 19, 71–91, https://doi.org/10.5194/bg-19-71-2022, 2022.

Tedersoo, L., Bahram, M., Põlme, S., Kõljalg, U., Yorou, N. S., Wijesundera, R., Ruiz, L. V., Vasco-Palacios, A. M., Thu, P. Q., Suija, A., Smith, M. E., Sharp, C., Saluveer, E., Saitta, A., Rosas, M., Riit, T., Ratkowsky, D., Pritsch, K., Põldmaa, K., Piepenbring, M., Phosri, 970 C., Peterson, M., Parts, K., Pärtel, K., Otsing, E., Nouhra, E., Njouonkou, A. L., Nilsson, R. H., Morgado, L. N., Mayor, J., May, T. W., Majuakim, L., Lodge, D. J., Lee, S. S., Larsson, K.-H., Kohout, P., Hosaka, K., Hiiesalu, I., Henkel, T. W., Harend, H., dong Guo, L., Greslebin, A., Grelet, G., Geml, J., Gates, G., Dunstan, W., Dunk, C., Drenkhan, R., Dearnaley, J., Kesel, A. D., Dang, T., Chen, X., Buegger, F., Brearley, F. Q., Bonito, G., Anslan, S., Abell, S., and Abarenkov, K.: Global diversity and geography of soil fungi, Science, 346, 1256 688, https://doi.org/10.1126/science.1256688, 2014.

975 Tedersoo, L., Bahram, M., Zinger, L., Nilsson, R. H., Kennedy, P. G., Yang, T., Anslan, S., and Mikryukov, V.: Best practices in metabarcoding of fungi: From experimental design to results, Mol Ecol, 31, 2769–2795, https://doi.org/10.1111/mec.16460, 2022.

Tobo, Y., Adachi, K., DeMott, P. J., Hill, T. C. J., Hamilton, D. S., Mahowald, N. M., Nagatsuka, N., Ohata, S., Uetake, J., Kondo, Y., and Koike, M.: Glacially sourced dust as a potentially significant source of ice nucleating particles, 12, 253–258, https://doi.org/10.1038/s41561-019-0314-x.

980 Tobo, Y., Prenni, A. J., DeMott, P. J., Huffman, J. A., McCluskey, C. S., Tian, G., Pöhlker, C., Pöschl, U., and Kreidenweis, S. M.: Biological aerosol particles as a key determinant of ice nuclei populations in a forest ecosystem, J Geophys Res: Atmos, 118, 10,100–10,110, https://doi.org/10.1002/jgrd.50801, 2013.

Tobo, Y., Adachi, K., Kawai, K., Matsui, H., Ohata, S., Oshima, N., Kondo, Y., Hermansen, O., Uchida, M., Inoue, J., and Koike, M.: Surface warming in Svalbard may have led to increases in highly active ice-nucleating particles, Commun Earth Environ, 5, 516, 985 https://doi.org/10.1038/s43247-024-01677-0, 2024.

Tsumuki, H., Yanai, H., and Aoki, T.: Identification of ice-nucleating active fungus isolated from the gut of the rice stem borer, Chilo suppressalis Walker (Lepidoptera: Pyralidae) and a search for ice-nucleating active Fusarium species, Japanese Journal of Phytopathology, 61, 334–339, 1995.

Twohy, C. H., McMeeking, G. R., DeMott, P. J., McCluskey, C. S., Hill, T. C. J., Burrows, S. M., Kulkarni, G. R., Tanarhte, M., Kafle, D. N., and Toohey, D. W.: Abundance of fluorescent biological aerosol particles at temperatures conducive to the formation of mixed-phase and cirrus clouds, Atmos Chem Phys, 16, 8205–8225, https://doi.org/10.5194/acp-16-8205-2016, 2016.

Vali, G.: Quantitative Evaluation of Experimental Results an the Heterogeneous Freezing Nucleation of Supercooled Liquids, J. Atmos. Sci., 28, 402–409, https://doi.org/10.1175/1520-0469(1971)028<0402:qeoera>2.0.co;2, 1971.

Vogel, F., Adams, M. P., Lacher, L., Foster, P. B., Porter, G. C. E., Bertozzi, B., Höhler, K., Schneider, J., Schorr, T., Umo, N. S., Nadolny, J., Brasseur, Z., Heikkilä, P., Thomson, E. S., Büttner, N., Daily, M. I., Fösig, R., Harrison, A. D., Keskinen, J., Proske, U., Duplissy, J., Kulmala, M., Petäjä, T., Möhler, O., and Murray, B. J.: Ice-nucleating particles active below $-24\,°C$ in a Finnish boreal forest and their relationship to bioaerosols, Atmos Chem Phys, 24, 11 737–11 757, https://doi.org/10.5194/acp-24-11737-2024, 2024.

Vu, D., Groenewald, M., de Vries, M., Gehrmann, T., Stielow, B., Eberhardt, U., Al-Hatmi, A., Groenewald, J., Cardinali, G., Houbraken, J., Boekhout, T., Crous, P., Robert, V., and Verkley, G.: Large-scale generation and analysis of filamentous fungal DNA barcodes boosts coverage for kingdom fungi and reveals thresholds for fungal species and higher taxon delimitation, Stud Mycol, 92, 135–154, https://doi.org/10.1016/j.simyco.2018.05.001, 2019.

Welti, A., Müller, K., Fleming, Z. L., and Stratmann, F.: Concentration and variability of ice nuclei in the subtropical maritime boundary layer, Atmos Chem Phys, 18, 5307–5320, https://doi.org/10.5194/acp-18-5307-2018, 2018.

Wex, H., Huang, L., Zhang, W., Hung, H., Traversi, R., Becagli, S., Sheesley, R. J., Moffett, C. E., Barrett, T. E., Bossi, R., Skov, H., Hünerbein, A., Lubitz, J., Löffler, M., Linke, O., Hartmann, M., Herenz, P., and Stratmann, F.: Annual variability of ice-nucleating particle concentrations at different Arctic locations, Atmos Chem Phys, 19, 5293–5311, https://doi.org/10.5194/acp-19-5293-2019, 2019.

Wieland, F., Bothen, N., Schwidetzky, R., Seifried, T. M., Bieber, P., Pöschl, U., Meister, K., Bonn, M., Fröhlich-Nowoisky, J., and Grothe, H.: Aggregation of ice-nucleating macromolecules from *Betula pendula* pollen determines ice nucleation efficiency, Biogeosciences, 22, 103–115, https://doi.org/10.5194/bg-22-103-2025, 2025.

Wright, T. P., Hader, J. D. and. McMeeking, G. R., and Petters, M. D.: High Relative Humidity as a Trigger for Widespread Release of Ice Nuclei, Aerosol Sci Tech, 48, i–v, https://doi.org/10.1080/02786826.2014.968244, 2014.

Wu, R., Song, Y., Head, J. R., Katz, D. S., Peay, K. G., Shedden, K., and Zhu, K.: Fungal spore seasons advanced across the US over two decades of climate change, bioRxiv, pp. 2024–10, 2024.

Xie, S., Liu, X., Zhao, C., and Zhang, Y.: Impact of ice nucleation parameterizations on CAM5 simulated arctic clouds and radiation: A sensitivity study, AIP Conference Proceedings, 1527, 747–750, https://doi.org/10.1063/1.4803378, 2013.

Xie, W., Li, Y., Bai, W., Hou, J., Ma, T., Zeng, X., Zhang, L., and An, T.: The source and transport of bioaerosols in the air: A review, Front Environ Sci Eng, 15, https://doi.org/10.1007/s11783-020-1336-8, 2020.

Yamamoto, N., Bibby, K., Qian, J., Hospodsky, D., Rismani-Yazdi, H., Nazaroff, W. W., and Peccia, J.: Particle-size distributions and seasonal diversity of allergenic and pathogenic fungi in outdoor air, 6, 1801–1811, https://doi.org/10.1038/ismej.2012.30, 2012.

Yue, S., Ren, L., Song, T., Li, L., Xie, Q., Li, W., Kang, M., Zhao, W., Wei, L., Ren, H., Sun, Y., Wang, Z., Ellam, R. M., Liu, C.-Q., Kawamura, K., and Fu, P.: Abundance and Diurnal Trends of Fluorescent Bioaerosols in the Troposphere over Mt. Tai, China, in Spring, J Geophys Res: Atmos, 124, 4158–4173, https://doi.org/10.1029/2018JD029486, 2019.

Yue, S., Li, L., Xu, W., Zhao, J., Ren, H., Ji, D., Li, P., Zhang, Q., Wei, L., Xie, Q., Pan, X., Wang, Z., Sun, Y., and Fu, P.: Biological and Nonbiological Sources of Fluorescent Aerosol Particles in the Urban Atmosphere, Environ Sci Technol, 56, 7588–7597, https://doi.org/10.1021/acs.est.1c07966, 2022.

Zelinka, M. D., Myers, T. A., McCoy, D. T., Po-Chedley, S., Caldwell, P. M., Ceppi, P., Klein, S. A., and Taylor, K. E.: Causes of Higher Climate Sensitivity in CMIP6 Models, Geophys Res Lett, 47, e2019GL085 782, https://doi.org/10.1029/2019GL085782, e2019GL085782 10.1029/2019GL085782, 2020.

Zoberi, M.: Effect of temperature and humidity on ballistospore discharge, Trans Br Mycol Soc, 47, 109–114, https://doi.org/10.1016/S0007-1030 1536(64)80085-1, 1964.

Šantl Temkiv, T., Sahyoun, M., Finster, K., Hartmann, S., Augustin-Bauditz, S., Stratmann, F., Wex, H., Clauss, T., Nielsen, N. W., Sørensen, J. H., Korsholm, U. S., Wick, L. Y., and Karlson, U. G.: Characterization of airborne ice-nucleation-active bacteria and bacterial fragments, Atmos Environ, 109, 105–117, https://doi.org/10.1016/j.atmosenv.2015.02.060, 2015.

Šantl Temkiv, T., Lange, R., Beddows, D., Rauter, U., Pilgaard, S., Dall'Osto, M., Gunde-Cimerman, N., Massling, A., and Wex, H.: Bio-1035 genic Sources of Ice Nucleating Particles at the High Arctic Site Villum Research Station, Environ Sci Technol, 53, 10 580–10 590, https://doi.org/10.1021/acs.est.9b00991, 2019.